

공학석사학위논문

Identification of Statistical Model of
Vehicular Live Load in Long Span Bridges
using WIM data

WIM data 를 이용한
장경간교량 차량활하중 확률모형 추정

2015 년 2 월

서울대학교 대학원

건설환경공학부

김 중 현

Abstract

In this paper the statistical model of the vehicular live load on long span bridges reflecting Korean traffic pattern was identified. Traffic jams, which are assumed for live load model on long span bridges, do not always occur in reality. The assumption may lead to excessive conservatism. To reflect actual traffic patterns, driving situations other than traffic jams were investigated using recently measured traffic data from six different sites in Korea. An extrapolation method using Cramer's asymptotic solution was proposed to estimate maximum load distribution. A method developing multiple presence factors appropriate for long span bridges was discussed. The statistical characteristics of live the load model (Hwang, 2012) was estimated. Bias factor was not uniform according to influence length due to different decreasing rate of load. Site-to-site variability also needed to be considered. A new live load model for long span bridges incorporating the decreasing rates and site-to-site variability was proposed. The lane load was classified into two groups: normal and heavy traffic sites. Load models for influence line length and span length were proposed respectively. The statistical characteristics of the proposed load model and load effects were identified.

Key words: vehicular live load model on long span bridge, statistical model, Cramer's asymptotic solution, WIM data, multiple presence factor

Student number: 2013-20924

Contents

Abstract	i
Contents	ii
List of Figures	v
List of Tables.....	vii
1. Introduction.....	1
1.1 Background	1
1.2 Objectives.....	4
1.3 Organization of the thesis.....	4
2. Basic Statistics for Statistical Model Identification	6
2.1 Basic Theory of Statistics.....	6
2.1.1 Random Variables	6
2.2 Probability Distribution of Extremes	8
2.2.1 Exact Distribution	9
2.2.2 Asymptotic Distribution	11
2.2.3 The Three Asymptotic Forms.....	14
2.3 Probability Paper.....	17
2.3.1 Empirical CDF	18
2.3.2 Normal Probability Paper.....	18

2.3.3 Gumbel Probability Paper	20
3. International Design Live Load Model.....	22
3.1 KBDC – LSD(2012)	23
3.2 DGCSB (2006).....	25
3.3 AASHTO LRFD (2012).....	27
3.4 ASCE Loading (1981).....	28
4. Drive Analysis.....	30
4.1 Introduction.....	30
4.2 Weight-In-Motion data.....	33
4.2.1 WIM locations.....	33
4.2.2 Data Scrubbing.....	34
4.2.3 Data generation	35
4.2.4 Statistics of collected data.....	37
4.3 Drive Analysis.....	40
4.3.1 Method	40
4.3.2 Results.....	41
4.4 Multiple Presence Factor	43
4.4.1 Method	43
4.4.2 Proposal of multiple presence factor for bridges with long spans.....	44
5. Statistical Model of Live Load for Long span Bridges	46

5.1 Estimation of the Maximum Load	47
5.1.1 Estimation by return period load.....	47
5.1.2 Estimation by maximum load distribution	51
5.1.3 Estimation using Cramer's asymptotic solution.....	54
5.2 Statistical Characteristics of Vehicular Live Load	59
5.2.1 Design live load model.....	59
5.2.2 Bias factor of the design lane load model	60
5.3 Proposal of New Lane Load Model	65
5.3.1 Lane load model	65
5.3.2 Statistical characteristics of live load for long spans	70
5.4 Summary	73
6. Conclusions	75
References	77
초 록	81

List of Figures

Figure 2.1 Normal probability paper and cumulative distribution function($\mu_x = 5, \sigma_x = 1$)..	19
Figure 2.2 Gumbel probability paper and cumulative distribution function ($u_n = 5, \alpha_n = 1$)..	21
Figure 3.1 Design truck load (KBDC, 2012).....	24
Figure 3.2 DB, DL Load Model (DGCSB, 2006)	26
Figure 3.3 Characteristics of the Design Truck (AASHTO, 2012).....	27
Figure 3.4 ASCE Loading on Log Scale (Buckland 1981; quoted from Lutomirska, 2009)..	29
Figure 4.1 Critical loading. Traffic jam scenario [Nowak et al. (2010)]	31
Figure 4.2 Traffic scenario (Hwang, 2012)	31
Figure 4.3 Average daily traffic of each vehicle type and truck traffic in one lane	38
Figure 4.4 Average GVW of each vehicle type	39
Figure 4.5 Vehicle position of a certain time	40
Figure 4.6 Multi-lane simulation.....	43
Figure 4.7 Comparison of the multiple presence factors (The KDBC (2012)* is normalized to 1.0 for two lanes).....	45
Figure 5.1 Maximum UDL estimation using the extrapolation method of Nowak (1999)..	50
Figure 5.2 Maximum UDL estimation using the extrapolation method of Lee (2014)	53
Figure 5.3 Estimated maximum UDL distribution using Cramer’s asymptotic solution.....	58
Figure 5.4 Comparison of extrapolation method between the proposed method and Lee’s (2014) method	58
Figure 5.5 Design truck load (KBDC, 2012).....	59
Figure 5.6 Daily maximum UDL distribution	60
Figure 5.7 The mean value of 100-year maximum UDL	64

Figure 5.8 Bias factor (mean to nominal value of UDL).....64

Figure 5.9 Average of normal and heavy traffic lane load.....66

Figure 5.10 Proposed lane load and the mean of 100-year max. UDL.....67

Figure 5.11 Comparison of proposed model with other sites70

Figure 5.12 Bias factor of proposed lane load model(normal, heavy traffic)71

Figure 5.13 Coefficient of variation of lane load71

List of Tables

Table 3.1 Design lane load (KBDC, 2012).....	24
Table 3.2 Multiple Presence Factors (KBDC, 2012).....	24
Table 3.3 Coefficient of variation of load effects (Hwang et al., 2012).	25
Table 3.4 DB load (DGCSB, 2006).....	26
Table 3.5 DL load (DGCSB, 2012).....	26
Table 3.6 Multiple Presence Factors (AASHTO LRFD, 2012).....	28
Table 4.1 WIM measurement locations.....	34
Table 4.2. Twelve vehicle type classifications (MLTM, 2012).....	35
Table 4.3 Properties of the generated data.....	36
Table 4.4 WIM data after scrubbing and data generation.....	37
Table 4.5 Speed statistics of WIM data.....	39
Table 4.6 The average of UDL (kN/m).....	42
Table 4.7 The standard deviation of UDL (kN/m).....	42
Table 4.8 The maximum value of UDL (kN/m).....	42
Table 4.9 Multiple presence factors.....	45
Table 5.1 Number of events and probability according to time period [Nowak's (1999) method].....	49
Table 5.2 Maximum UDL estimation [Nowak's (1999) extrapolation method].....	50
Table 5.3 Comparison of the measured and estimated maximum UDL of GC (500m).....	58
Table 5.4 Design lane load (KBDC, 2012).....	59
Table 5.5 Daily maximum UDL distribution (Gumbel distribution).....	61
Table 5.6 Estimated parent UDL distribution (Normal distribution).....	62

Table 5.7 Estimated 100-year maximum UDL distribution (Gumbel distribution).....62

Table 5.8 Estimated 100-year maximum UDL distribution (continue)63

Table 5.9 Proposed lane load, $w = A \times \left(\frac{100}{L}\right)^B$ 67

Table 5.10 Design lane load (KBDC, 2014 (under revision))68

1. Introduction

1.1 Background

Bridge design codes in many countries have been changed from Allowable Stress Design (ASD) to the probability-based Limit State Design (LSD). ASD, which was a common design method in the past and still in use today, is based on a deterministic method. The allowable stress is set by safety factors to account for uncertainty and provide a safety margin. However, the safety factor has been determined empirically, and the effects from different loads are considered simultaneously. It is, therefore, inadequate to provide a uniform level of safety. In contrast, the probability-based LSD defines possible limit states and calculates safety level (defined in reliability index) based on reliability theory. It accounts for the different variability levels of various loads and resistances independently. Therefore, a more consistent reliability level can be attained. ISO2394 (ISO, 1998), Eurocode (CEN, 2001), and AASHTO LRFD (AASHTO, 2007) have already established their reliability-based limit state design codes. In Korea, the Korea Bridge Design Engineering Research Center has conducted long-term research to introduce limit state design to the Korea Bridge Design Code (KBDC), and consequently the Korea Bridge Design Code – Limit State Design(KBDC-LSD)(MLTM, 2012) was established.

It is essential to obtain a sufficient amount and quality of statistical data for the reliability analysis. And it is also important to identify an appropriate statistical model of loads and resistances from the statistical data. Vehicular live load is one of

the most important components in bridge design and evaluation. Inadequate knowledge of live load may lead to uneconomical or unsafe design. In America, Nowak developed a statistical model of vehicular live load using two weeks Ontario truck survey data (Nowak, 1993; Nowak and Hong, 1991; Hwang and Nowak 1991). The current American vehicular live load model, HL93, was developed in Nowak's (1999) research. Maximum expected values for various time periods were calculated, and the design live load model was developed based on 75-year maximum load effects. The statistical data from two-week periods are relatively short compared to the design life and, therefore, statistical parameters were estimated using an extrapolation method. However, relatively short-term truck survey data may not be enough to account for the long-term variation. In addition, heavy vehicles may avoid the survey station intentionally or control lifting axles.

The WIM (Weight-In-Motion) system collects axle weights during drive situation. An early version of WIM included considerable amount of errors or measured only low-speed traffic data. Nowak et al. (1993) used low-speed (8-16km/h) WIM data. However, the WIM technology has greatly improved in recent years and more reliable and long-term statistical traffic data are now available. High-speed WIM systems can measure traffic data at normal highway speeds without driver's knowledge. Using recent WIM data of 35 million trucks, Nowak and Rakoczy (2013) reviewed statistical parameters of AASHTO LRFD live load moments according to the same procedure used by Nowak (1999). Moses (2001) used WIM data and presented an equation that computes the maximum weight for bridge evaluation.

In Korea, Koh (1998) reviewed vehicular live load models in America, the United Kingdom, Japan and Germany and developed a live load model using domestic WIM data. As a result of a long-term project of the Korea Bridge Design Engineering Research Center, Hwang (2008) developed a live load model for KBDC(2012) using domestic WIM data.

The statistical models of live load stated above are limited to short- and medium-span bridges. The HL-93 live load model was developed for 10 ~ 200ft span bridges (Nowak, 1999). For long spans, the ASCE model (Buckland 1981) was developed in the 1980s. And Nowak et al. (2010) investigated recent WIM data and concluded that HL-93 is appropriate for long span bridges. In Korea, the live load model for long span bridges was presented in the Korean Design Guideline of Cable Steel Bridge (2006), but this is an ASD method. KBDC (2012) provides the live load model without limitation of span length, but the model was not extensively investigated for bridges longer than 200m. Hwang (2012) developed a new live load model for long span cable bridges, and the model is now under review for new revision of KDBC. The statistical characteristics of the live load model, however, have not been clearly stated.

The models of Nowak et al. (2010) and Hwang (2012) were developed for assumed traffic jam situation. They do not incorporate the probability of occurrence but assume the occurrence of traffic jams, which may contribute to artificial bias. Lee (2014) estimated the bias factor of the live load model proposed by Hwang (2012), and the estimated bias factor was excessive compared to the bias factor of

the KBDC(2012). Therefore, real traffic – not hypothetical traffic - should be considered.

In contrast with short- and medium live load model, multiple presence factors should be considered in different way for long span live load model. For short- and medium- span live load model, probability of side-by-side multiple truck occurrence is applied to heavy trucks (Nowak, 1999; Hwang, 2008). For long span bridges, however, multiple vehicles including not only heavy trucks but also other small vehicles should be considered. Therefore multiple presence factors which are appropriate for long span bridges should be developed.

1.2 Objectives

The objective of this study is to identify a statistical model of vehicular live load on long span bridges reflecting Korean traffic patterns. To reflect actual traffic patterns, driving situations other than traffic jams were investigated using recently measured traffic data. The extrapolation method is compared to identify an exact statistical model. The multiple presence factor appropriate to long span bridges was considered. Finally, a new live load model reflecting actual traffic patterns and statistical characteristics of it was proposed.

1.3 Organization of the thesis

This paper is organized as follow. Chapter 1 presents the background, purpose,

and organization of this study. Chapter 2 presents basic knowledge of statistics for understanding this thesis. Chapter 3 reviews the existing live load models. Live load models, multi-lane consideration, dynamic effects, and statistical characteristics are presented. Chapter 4 describes the procedure of drive analysis, analyzing the actual traffic patterns. WIM data is presented and multiplication factors are considered in this chapter. Chapter 5 presents statistical models of live load model for long span bridges and a new model is proposed.

2. Basic Statistics for Statistical Model Identification

2.1 Basic Theory of Statistics

2.1.1 Random Variables

(1) Definition of random variables

Random variable is a variable whose values are not fixed for the same event under the same condition but distributed around representative value. Random variable is defined by certain regulation or function in sample space and divided into discrete random variable and continuous random variable. Discrete random variable is a random variable with finite elements or countable infinite elements and continuous random variable is a random variable whose values can be any value in a certain interval.

(2) Probabilistic function

Probabilistic function is a representation of probability value which corresponds to random variable in a function form and can be separated into: Probabilistic mass function(PMF), Probabilistic density function(PDF), Cumulative distribution function(CDF). PMF and PDF is defined by discrete random variable and continuous random variable each, and CDF is defined by both.

PMF $p_X(x)$ about discrete random variable X and PDF $f_X(x)$ about continuous random variable X are defined as follows:

$$p_X(x) = P[X = x] \quad (2.1a)$$

$$f_X(x) = P[x \leq X \leq x + dx] \quad (2.1b)$$

CDF $F_X(x)$ about discrete random variable and continuous random variable is defined as:

$$F_X(x) = P[X \leq x] = \sum_{x_i \leq x} p_X(x_i) \quad (2.2a)$$

$$F_X(x) = P[X \leq x] = \int_{-\infty}^x f_X(u) du \quad (2.2b)$$

(3) Statistical characteristics of a random variable

Statistical characteristic of a random variable would be described completely if the form of the distribution function and the associated parameters are specified. In practice, however, the distribution may not be known. Instead, approximate description of a random variable such as mean value, variance, and standard deviation can be used. Even when the distribution function is known, these quantities remain useful.

Mean value of random variable X (μ_X), by discrete random variable and continuous random variable, expressed as 1st moment:

$$\mu_X = E[X] = \sum_{x_i} x_i p_X(x_i) \quad (2.3a)$$

$$\mu_X = E[X] = \int_{-\infty}^{\infty} x f_X(x) dx \quad (2.3b)$$

Variance and standard deviation of random variable X (V_X and σ_X) can be derived using 2nd moment

$$V_X = E[X^2] - (E[X])^2 \quad (2.4a)$$

$$\sigma_X = \sqrt{V_X} = \sqrt{E[X^2] - (E[X])^2} \quad (2.4b)$$

Coefficient of variation of random variable X (δ_X) is used to measure variance of random variable, and defined as ratio of standard deviation to mean value

$$\delta_X = \frac{\sigma_X}{\mu_X} \quad (2.5)$$

2.2 Probability Distribution of Extremes

In bridge design the maximum load distribution is of concern, rather than the entire load distribution itself. The maximum load distribution can be developed from extreme distribution. More detailed information about the statistics of extremes can be found in textbook (Ang et. al, 1984). The largest and smallest values from samples of size n are also random variables and therefore they have probability distributions of their own. These distributions can be expected to be related to the distribution of the initial variate.

2.2.1 Exact Distribution

Let X be the initial random variable with known initial distribution function $F_X(x)$. Consider sets of samples of size n taken from the population. Each sample will be a set of observations (x_1, x_2, \dots, x_n) representing respectively the first, second, ..., n -th observed values. Then we may assume each value can be considered as random variables (X_1, X_2, \dots, X_n) . The extreme values from a sample size n are the maximum and minimum values. Let the random variables of extreme values are Y_n, Y_1 defined as equation (2.6).

$$Y_n = \max(X_1, X_2, \dots, X_n) \quad (2.6a)$$

$$Y_1 = \min(X_1, X_2, \dots, X_n) \quad (2.6b)$$

If Y_n is larger than a value y , all the sample random variables X_1, X_2, \dots, X_n must be less than y . Assume X_1, X_2, \dots, X_n are statistically independent and identically distributed as the initial variate X .

$$F_{X_1}(x_1) = F_{X_2}(x_2) = \dots = F_{X_n}(x_n) = F_X(x) \quad (2.7)$$

The cumulative distribution function of Y_n and the corresponding probability density function are derived as equations (2.8) and (2.9)

$$\begin{aligned}
F_{Y_n}(y) &= P(Y_n \leq y) \\
&= P(X_1 \leq y, X_2 \leq y, \dots, X_n \leq y) \\
&= [F_X(y)]^n
\end{aligned} \tag{2.8}$$

$$\begin{aligned}
f_{Y_n}(y) &= \frac{\partial F_{Y_n}(y)}{\partial y} \\
&= n[F_X(y)]^{n-1} f_X(y)
\end{aligned} \tag{2.9}$$

Likewise if Y_1 less than a value y , the cumulative distribution function of Y_1 is

$$\begin{aligned}
1 - F_{Y_1}(y) &= P(Y_1 \geq y) \\
&= P(X_1 \geq y, X_2 \geq y, \dots, X_n \geq y) \\
&= [1 - F_X(y)]^n
\end{aligned}$$

Therefore, the cumulative distribution function of Y_1 and the corresponding probability density function are

$$F_{Y_1}(y) = 1 - [1 - F_X(y)]^n \tag{2.10}$$

$$f_{Y_1}(y) = n[1 - F_X(y)]^{n-1} f_X(y) \tag{2.11}$$

The Equation (2.8) through (2.11) are the exact probability distributions of the extremes from samples of size n taken from a population X . And these

distributions depend on the initial distribution $F_X(x)$ of the population and also on the sample size n . The distributions of Y_n and Y_1 are generally difficult to obtain or derive in analytic form.

2.2.2 Asymptotic Distribution

As $n \rightarrow \infty$, $F_{Y_n}(y)$ and $F_{Y_1}(y)$ converges to a particular functional asymptotic form. The asymptotic form of an extremal distribution depends largely on the tail behavior of the initial distribution, and the central portion of the initial distribution has little influence on the asymptotic form. The analytical derivation of the appropriate asymptotic extremal distribution given the distribution of an initial variate is facilitated by the method of Cramer.

Consider the extremal distribution for the largest value from an initial variate X . Following Cramer (1946), define the transformed random variable ξ_n .

$$\xi_n = n[1 - F_X(Y_n)] \quad (2.12)$$

Then,

$$\begin{aligned} F_{\xi_n}(\xi) &= P(\xi_n \leq \xi) = P\{n[1 - F_X(Y_n)] \leq \xi\} = P\left[F_X(Y_n) \geq 1 - \frac{\xi}{n}\right] \\ &= P\left[Y_n \geq F_X^{-1}\left(1 - \frac{\xi}{n}\right)\right] \\ &= 1 - F_{Y_n}\left[F_X^{-1}\left(1 - \frac{\xi}{n}\right)\right] = 1 - \left\{F_X\left[F_X^{-1}\left(1 - \frac{\xi}{n}\right)\right]\right\}^n \\ &= 1 - \left(1 - \frac{\xi}{n}\right)^n \end{aligned} \quad (2.13)$$

As $n \rightarrow \infty$,

$$F_{\xi_n}(\xi) = 1 - e^{-\xi} \quad (2.14)$$

The corresponding asymptotic PDF is

$$f_{\xi_n}(\xi) = e^{-\xi} \quad (2.15)$$

From equation (2.12) and (2.14)

$$Y_n = F_X^{-1}\left(1 - \frac{\xi_n}{n}\right) \quad (2.16)$$

Define $g(y)$ as follow

$$g(y) = n[1 - F_X(Y_n)] \quad (2.17)$$

Then,

$$P(Y_n \leq y) = P[\xi_n > g(y)] \quad (2.18)$$

Therefore, the asymptotic CDF and PDF of Y_n is

$$F_{Y_n}(y) = 1 - F_{\xi_n}[g(y)] = \exp[-g(y)] \quad (2.19)$$

$$f_{Y_n}(y) = -\frac{dg(y)}{dy} \exp[-g(y)] \quad (2.20)$$

Consider standard normal initial variate. The transformed variate of equation (2.12)

is

$$\xi_n = \frac{n}{\sqrt{2\pi}} \int_{Y_n}^{\infty} e^{-(1/2)z^2} dz \quad (2.21)$$

Integrating by parts, with $u = \frac{1}{z}$ and $dv = ze^{-(1/2)z^2} dz$

$$\xi_n = \frac{n}{\sqrt{2\pi}} \frac{1}{Y_n} e^{-(1/2)Y_n^2} \left[1 + o\left(1/Y_n^2\right) \right] \quad (2.22)$$

Cramer(1946) gives the following asymptotic solution for Y_n as $n \rightarrow \infty$

$$\xi_n = \sqrt{2 \ln n} - \frac{\ln \ln n + \ln 4\pi}{2\sqrt{2 \ln n}} - \frac{\ln \xi_n}{\sqrt{2 \ln n}} \quad (2.23)$$

Denoting

$$u_n = \sqrt{2 \ln n} - \frac{\ln \ln n + \ln 4\pi}{2\sqrt{2 \ln n}}, \quad \alpha_n = \sqrt{2 \ln n} \quad (2.24)$$

The ξ_n becomes

$$\xi_n = \exp\{-\alpha_n(Y_n - u_n)\} \quad (2.25)$$

From equation (2.19), the CDF of Y_n becomes

$$F_{Y_n}(y) = \exp[-\exp\{-\alpha_n(y - u_n)\}] \quad (2.26)$$

2.2.3 The Three Asymptotic Forms

The extreme value distribution depends largely on the tail behavior of initial distribution in the direction of extreme. There are three type of extreme value distribution according to the Gumbel's classification. The three type of the largest extreme values distribution and the mean and standard deviation of them are as follow.

(1) The Type I Asymptotic Form

If an initial distribution with an exponentially decaying tail in the direction of extreme, the extreme value distribution will converge to the Type I asymptotic form.

The largest extreme value distribution are

$$F_{X_n}(x) = \exp[-\exp\{-\alpha_n(x - u_n)\}] \quad (2.27a)$$

$$f_{X_n}(x) = \alpha_n \exp\{-\alpha_n(x - u_n)\} \exp[-\exp\{-\alpha_n(x - u_n)\}] \quad (2.27b)$$

$$\mu_{X_n} = u_n + \frac{\gamma}{\alpha_n}, \quad \sigma_{X_n}^2 = \frac{\pi^2}{6\alpha_n^2} \quad (2.27c)$$

The parameter u_n is the location the parameters which is the most probable values of the extreme variate X_n . And the parameter α_n are the shape parameters which is an inverse measure of dispersion of the extreme variate X_n . γ is the Euler constant $\gamma = 0.55716\dots$.

(2) The Type II Asymptotic Form

If the initial distribution has polynomial tail in the direction of extreme, the extreme value distribution will converge to the Type II asymptotic distribution form.

$$F_{X_n}(x) = \exp\left\{-\left(\frac{\nu_n}{x}\right)^k\right\} \quad \text{for } x > 0, \nu_n > 0 \quad (2.28a)$$

$$f_{X_n}(x) = \frac{k}{\nu_n} \left(\frac{\nu_n}{x}\right)^{k+1} \exp\left\{-\left(\frac{\nu_n}{x}\right)^k\right\} \quad \text{for } x > 0, \nu_n > 0 \quad (2.28b)$$

$$\mu_{X_n} = \nu_n \Gamma\left(1 - \frac{1}{k}\right) \quad \text{for } k > 1 \quad (2.28c)$$

$$\sigma_{X_n}^2 = \nu_n \left[\Gamma\left(1 - \frac{2}{k}\right) - \Gamma^2\left(1 - \frac{1}{k}\right) \right] \quad \text{for } k > 2 \quad (2.28d)$$

The parameter ν_n is the location the parameters which is the most probable value of the extreme variate X_n . And the parameter k is the shape parameter which is an inverse measures of dispersion of each extreme variate X_n . $y = \Gamma(x)$ means the gamma function.

(3) The Type III Asymptotic Form

If the initial distribution has a finite upper or lower bound in the direction of extreme, the extreme value distribution will converge to the Type III asymptotic distribution form. The largest Type III asymptotic form are

$$F_{X_n}(x) = \exp\left\{-\left(\frac{\omega - x}{\omega - w_n}\right)^k\right\} \quad \text{for } x \leq \omega \quad (2.29a)$$

$$f_{X_n}(x) = \frac{k}{\omega - w_n} \left(\frac{\omega - x}{\omega - w_n}\right)^{k-1} \exp\left\{-\left(\frac{\omega - x}{\omega - w_n}\right)^k\right\} \quad \text{for } x \leq \omega \quad (2.29b)$$

$$\mu_{X_n} = \omega - (\omega - w_n) \Gamma\left(1 + \frac{1}{k}\right) \quad (2.29c)$$

$$\sigma_{X_n}^2 = (\omega - w_n)^2 \left[\Gamma\left(1 + \frac{2}{k}\right) - \Gamma^2\left(1 + \frac{1}{k}\right) \right] \quad (2.29c)$$

ω is the upper bound value of the initial variate X . The parameter w_n is the location the parameters which is the most probable value of the extreme variate X_n . And the parameter k is the shape parameter which is an inverse measures of dispersion of each extreme variate X_n .

2.3 Probability Paper

The vehicular live load is treated as a random variable and therefore we have to define the probability distribution of the live load. For the reliable design and evaluation, the most appropriate probability distribution of the live load should be identified. Graphic methods using probability paper are simple and useful way. Probability distribution can be estimated and maximum load can be estimated by extrapolation using the probability paper.

Based on the observable data, we can determine the distribution of the data empirically. We can construct the histogram of observed data and compare with theoretical probability density functions. Or we can use probability paper prepared for specific distributions. Probability papers are constructed such that a given probability paper is associated with a specific probability distribution. Observed data are plotted on the probability paper and are determined whether the data follow the distribution by their linearity, or lack of linearity. Therefore the probability papers are different according to the distributions and no other distribution satisfy linearity on different probability paper. There are many kinds of probability papers and the normal probability paper and the Gumbel probability paper are described here. More detailed information about the probability paper can be found in textbook(Ang et. al, 1975; Castilo, 1988).

2.3.1 Empirical CDF

Let (x_1, x_2, \dots, x_N) are N observed data arranged in increasing order. Then empirical cumulative distribution function are assigned to m -th value as follow.

$$F_{X_m} = \frac{m-a}{N+(1-2a)} \quad (2.30)$$

The a is parameter determining the plotting position and many different values of the a are introduced to different distributions(Castilo, 1988; Kang, 2008). However, the position based on Gumbel($a=0$) is known to have the theoretical attributes and the computational simplicity(Ang et al., 1975).

2.3.2 Normal Probability Paper

The normal probability paper is probability paper associated with the normal distribution. One axis is the variate X , and the other axis is the standard normal variate S of the variate X . If the variate X follows the normal distribution $X \sim N(\mu_X, \sigma_X)$, it will make a straight line according to the linear relation between two variate X and S

$$S = \frac{X - \mu_X}{\sigma_X} = \frac{1}{\sigma_X} X - \frac{\mu_X}{\sigma_X} \quad (2.31)$$

The CDF of the normal distribution and probability paper is compared in Figure 2.1

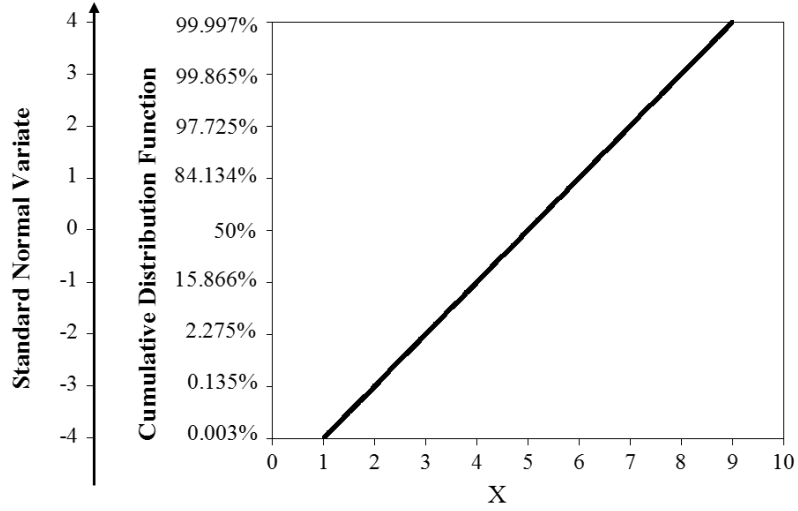


Figure 2.1 Normal probability paper and cumulative distribution function($\mu_x = 5$, $\sigma_x = 1$)

If there are N observed data (x_1, x_2, \dots, x_N) arranged in increasing order, we assign the empirical CDF $F_X(x_m)$ to the m -th smallest value x_m based on the equation (2.30) with $a = 0$. Then the S can be calculated by the inverse standard normal CDF.

$$S(x_m) = F_X^{-1}\{F_X(x_m)\} \quad (2.32)$$

If the plotted data follow the exact normal distribution, the observed data will be plotted in a line on the normal probability paper. Then, the probability distribution of the observed data can be identified by the linear equation (2.31). The mean is $-\frac{\alpha}{\beta}$

and the standard deviation is $\frac{1}{\beta}$, where the α and β are the y-intercept and the

slope, respectively. If the plotted data doesn't follow the exact normal distribution, the data does not make the straight line. An approximate normal distribution can be estimated drawing a straight line on the normal probability paper by error minimization.

2.3.3 Gumbel Probability Paper

The Gumbel probability paper is probability paper associated with the Gumbel distribution (the type I asymptotic distribution). One axis is the variate X , and the other axis is the standard extremal variate s . The standard extremal variate for the Gumbel distribution is written as equation (2.33)

$$s = \alpha_n(x_n - u_n) = \alpha_n x_n - \alpha_n u_n \quad (2.33)$$

If there are N observed data (x_1, x_2, \dots, x_N) arranged in increasing order, we assign the empirical CDF $F_X(x_m)$ to the m -th smallest value x_m based on the equation (2.30) with $a=0$. Then the S can be calculated by the inverse Gumbel CDF in equation (2.34). The CDF of the Gumbel distribution and probability paper is compared in Figure 2.2

$$S(x_m) = F_X^{-1}\{F_X(x_m)\} = -\ln[-\ln\{F_X(x_m)\}] \quad (2.34)$$

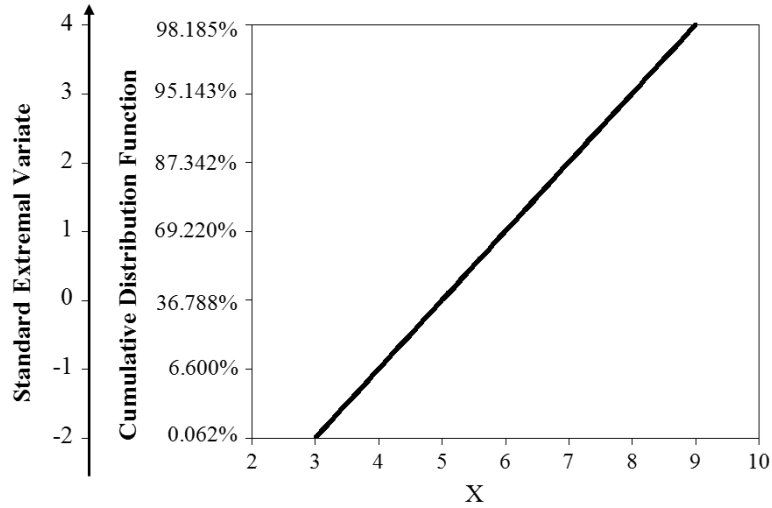


Figure 2.2 Gumbel probability paper and cumulative distribution function ($u_n = 5$, $\alpha_n = 1$)

If the plotted data follow the exact Gumbel distribution, the observed data will be plotted in a line on the Gumbel probability paper by the linear relation as (2.33). The location parameter(u_n) and shape parameter(α_n) can be derived from the y-intercept(α), and slope(β) of the line, that is, equation (2.34). The Gumbel probability paper with $u_n = 5$, $\alpha_n = 1$ is shown in Figure 2.2

$$u_n = -\frac{\alpha}{\beta}, \quad \alpha_n = -\frac{1}{\beta} \quad (2.34)$$

If the plotted data doesn't follow the exact Gumbel distribution, the data does not make the straight line. Then an approximate Gumbel distribution can be estimated drawing straight line on the Gumbel probability paper by error minimization.

3. International Design Live Load Model

Some of international vehicular live load models were compared in this chapter. KBDC-LSD(2012) and AASHTO LRFD(2012) are provided for general bridges with all spans, but DGCSB(2006) and ASCE(1981) are provided for bridge design especially for long spans. These live load models consist of concentrated loads and uniformly distributed loads. For short- and medium-span bridges, single or several heavily loaded truck effects governs the live load effect. If the span length increases, however, load effects by the mixture of vehicles may be important. For long span bridges, the load from different lanes is uniformly distributed to main components, and the influence of single truck decreases(Nowak et al., 2010). Therefore the live load for long span bridges can be modeled as lane load(Nowak et al, 2010; Hwang, 2012; Lee, 2014). The lane loads, except for AASHTO LRFD(2012), decrease when loaded lengths increase. It was reported that there was enough margin for long span bridges constructed in Korea, Seohae Grand Bridge, Youngjong Grand Bridge(DGCSB, 2006). Decreasing form of lane load model for loaded length is also used in BS 5400(2006). The design live loads, multi-lane considerations and dynamic effects are compared.

The statistical characteristics of LSD codes are also summarized. Bias factor (λ_{LL}) and COV (δ_{LL}) of the statistical model of the live load effect (Q_{LL}) can be defined by the following equation (Ellingwood et al., 1980):

$$\lambda_{LL} = \lambda_{C_{LL}} \cdot \lambda_{B_{LL}} \cdot \lambda_{A_{LL}} \quad (3.1a)$$

$$\delta_{LL} = \sqrt{\delta_{C_{LL}}^2 + \delta_{B_{LL}}^2 + \delta_{A_{LL}}^2} \quad (3.1b)$$

The influence factor, C_{LL} , reflects uncertainties arise from analysis which transforms load to load effect. The modeling parameter, B_{LL} , reflects the load modeling effects. A_{LL} is the structural load. The site-to-site variability and the effect of impact was considered as influence factor (Lee, 2014). Statistical characteristics of load effect, Q_{LL} , are determined considering all these effects together.

3.1 KBDC – LSD(2012)

The design live load model of the Korea Bridge Design Code – Limit State Design (KBDC) consists of design truck load, (Figure 3.1) and design lane load (Table 3.1). The extreme load effect is taken as the larger between ‘the effect of one design truck’ and ‘the effect of 75% of design truck combined with the effect of the design lane’. A value of 0.18 for n is provided in the KBDC (2012). Hwang(2012) proposed 0.15 for the new lane load model for long span cable bridges with the same truck load.

For multi-lane design, the live load model is multiplied by a number of design loaded lanes with the multiple presence factor. Table 3.2 presents the multiple

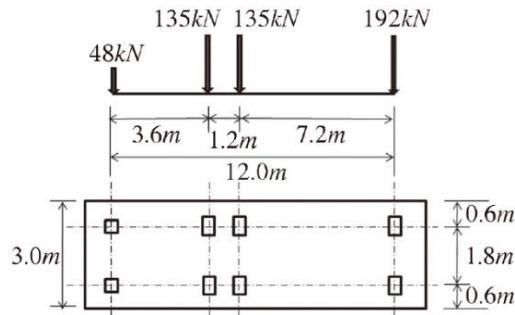


Figure 3.1 Design truck load (KBDC, 2012)

Table 3.1 Design lane load (KBDC, 2012)

$L \leq 60 \text{ m}$	$w = 12.7 \text{ (kN/m)}$
$L \geq 60 \text{ m}$	$w = 12.7 \times \left(\frac{60}{L}\right)^n \text{ (kN/m)}$

Table 3.2 Multiple Presence Factors (KBDC, 2012)

Number of Loaded Lanes	Multiple Presence Factors, m
1	1.0
2	0.9
3	0.8
4	0.7
≥ 5	0.65

presence factor. And a dynamic amplification factor of 0.25 is applied to the design truck.

Statistical characteristics of load effects of KBDC (2012) are stated in Hwang's study (Hwang, 2008; Hwang et al., 2012)'s study. The bias factor of load effects is 1.0 ~ 1.1 and the COV is 19%. Conservative value of COV, 20%, is used. The detail

COV calculation are presented in Table 3.3 and equation 3.2. Distribution type of live load effect is assumed as Gumbel distribution.

Table 3.3 Coefficient of variation of load effects (Hwang et al., 2012).

Effect	COV
Estimation	0.07
Analysis	0.1
Dynamic	0.1
Local	0.1

$$\delta_{LL} = \sqrt{0.07^2 + 0.1^2 + 0.1^2 + 0.1^2} = 0.19 \quad (3.2)$$

3.2 DGCSB (2006)

The Korean Design Guideline of Cable Steel Bridge (DGCSB) load consists of design truck load (DB load) and lane load (DL load) as shown in Figure 3.2. DB load (Table 3.4) is classified into three classes, and DL load (Table 3.5) is used for long span cable bridges. The larger force effect between DB and DL load should be taken. DGCSB load provides decreasing lane load for bridges with spans longer than 200m.

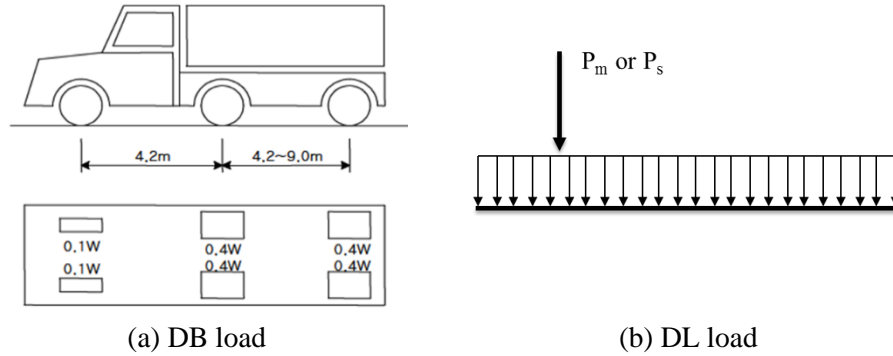


Figure 3.2 DB, DL Load Model (DGCSB, 2006)

Table 3.4 DB load (DGCSB, 2006)

Load	Total Weight (kN)	Front wheel weight (kN)	Rear wheel weight (kN)
DB-24	432	24	96
DB-18	324	18	72
DB-13.5	243	13.3	54

Table 3.5 DL load (DGCSB, 2012)

$L \leq 200\text{m}$	Concentrated load	$P_m = 108 \text{ kN}$ $P_s = 156 \text{ kN}$
	Distributed Lane Load	$w = 12.7 \text{ (kN/m)}$
$L \geq 200 \text{ m}$	Concentrated load	$P_m = 108 \text{ kN}$ $P_s = 156 \text{ kN}$
	Distributed Lane Load	$w = 12.7 \times \left(0.57 + \frac{300}{500 + L} \right) \text{ (kN/m)}$

Multi-lane load is evaluated using a multiple presence factor of 0.9 for three lanes and 0.75 for four or more lanes. Dynamic amplification factor (I) is considered in equation (3.3)

$$I = \frac{15}{40 + L} \leq 0.3 \quad (3.3)$$

3.3 AASHTO LRFD (2012)

The AASHTO HL-93 load model consists of a three-axle design truck (Figure 3.3), a pair of 111.2kN design tandem spaced 1.2m apart, and a uniformly distributed design lane load of 9.34kN/m per lane. The larger force effect of the following should be taken.

- 1) The effect of the design tandem combined with the effect of the design lane load,
or
- 2) The effect of one design truck, combined with the effect of the design lane load,
and
- 3) For negative moment between points of contraflexure under a uniform load on all spans, and reaction at interior piers only, 90 percent of the effect of two design trucks spaced a minimum of 50ft between the lead axle of one truck and the rear axle of the other truck, combined with 90 percent of the effect of the design lane load. The distance between the 32.0-kip axles of each truck shall be taken as 14.0 ft. The two design trucks shall be placed in adjacent spans to produce maximum force effects.

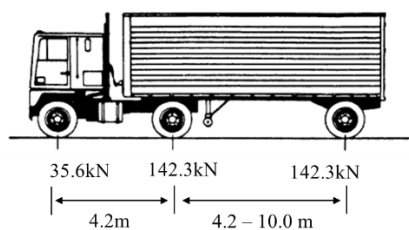


Figure 3.3 Characteristics of the Design Truck (AASHTO, 2012)

Table 3.6 Multiple Presence Factors (AASHTO LRFD, 2012)

Number of Loaded Lanes	Multiple Presence Factors, m
1	1.20
2	1.00
3	0.85
>3	0.65

The multiple presence factors are shown in Table 3.6, and a dynamic amplification factor of 0.33 is applied to the design truck. Statistical characteristics of load effects of HL-93 are presented in Nowak's (1999) study. The bias factors of load effects (moments and shears) are about 1.3 ~ 1.35 and that of live load with impact is presented as 1.10 ~ 1.20. The COV is presented as 18%, considering static live load, live load analysis factor, and dynamic load.

3.4 ASCE Loading (1981)

The ASCE Loading is a result of the studies performed by Peter G. Buckland, which was recommended by the American Society of Civil Engineers Committee on Loads and Forces on Bridges for long span bridges. ASCE (1981) specifies three levels of live load for highway bridges depending on the average percentage of heavy vehicles in traffic flow: 7.5%, 30%, and 100% heavy vehicles of the total vehicle population. "Heavy vehicles (HV)" were defined as buses and trucks over 12,000 lbs. In designing a new bridge, the expected trucks in the traffic must be estimated from traffic measurements. The ASCE model does not have any allowance for dynamic load. (quoted from Lutomirska, 2009)

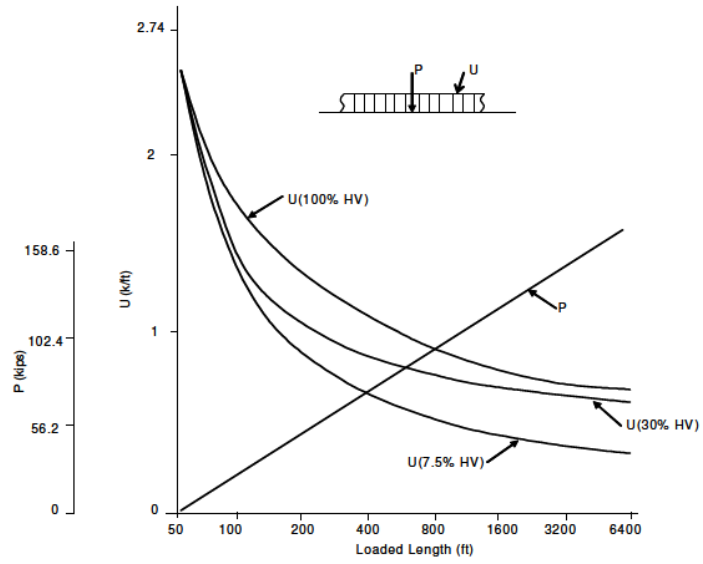


Figure 3.4 ASCE Loading on Log Scale (Buckland 1981; quoted from Lutomirska, 2009)

4. Drive Analysis

4.1 Introduction

For short- and medium-span bridges, single or several heavily loaded truck effects govern the live load effect. If the span length increases, however, load effects due to the mixture of vehicles may be important. For long span bridges, the load from different lanes is uniformly distributed to main components, and the influence of single truck decreases (Nowak et al., 2010). Therefore, the live load for long span bridges can be modeled as lane load (Nowak et al, 2010; Hwang, 2012; Lee, 2014).

The live load model for bridges with long spans was developed by Nowak et al. (2010), and it was concluded that the bias factor is less than 1.25 and the HL-93 can be applied to long span bridges. Based on WIM data obtained from NCHRP 12-76, traffic jam scenario was investigated as shown in Fig 4.1. Starting with the first truck, all consecutive trucks were added with a fixed headway distance (distance between the last axle of one truck and first axle of the following truck) of 7.6m until the total length exceeded the span length. Then the total weight of all trucks on a certain span length was calculated and divided by span length to obtain the average uniformly distributed load (UDL). Next, the first truck was deleted, and one or more trucks were added to cover the span length. The UDL distribution was identified by repeating the procedure. Only the most loaded lane was considered and motorcycles and small cars were omitted. The heaviest combination of vehicles over a 75-year period was calculated.

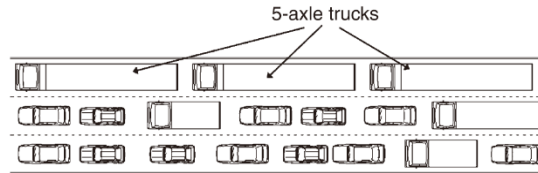
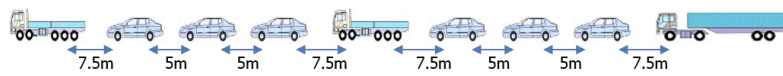
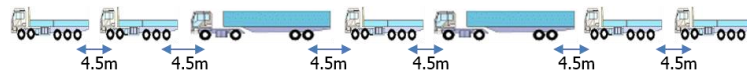


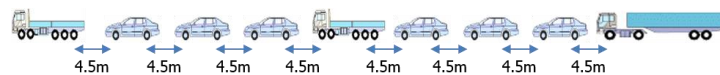
Figure 4.1 Critical loading. Traffic jam scenario [Nowak et al. (2010)]



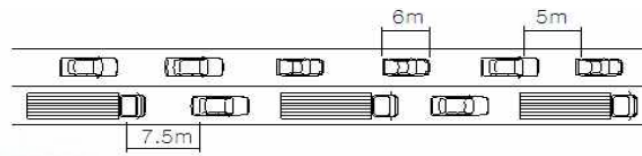
(a) Scenario 1-0



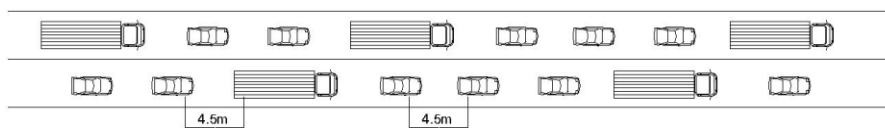
(b) Scenario 1-1



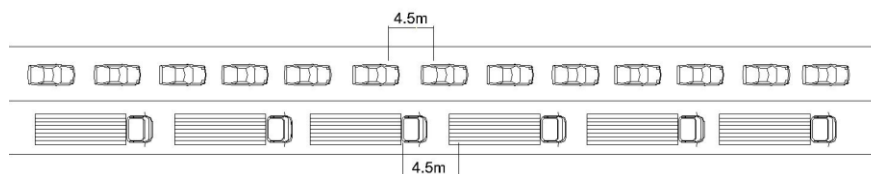
(c) Scenario 1-2



(d) Scenario 2-0



(e) Scenario 2-1



(f) Scenario 2-2

Figure 4.2 Traffic scenario (Hwang, 2012)

The vehicular live load on long span bridges, proposed by Hwang (2012), is based on presumed truck traffic jams as shown in Figure 4.2. Spacing between the last axle of one truck and first axle of the following truck was considered as 4.5m ~ 7.5m. Truck data are based on WIM data from six sites in Korea, and small vehicle data having 5.8kN/m in weight and 6m in length were generated with assumptions about traffic ratios (truck : small car = 3:7). Starting with the first truck all vehicles were arranged in a row according to the scenario until the total length reached a certain influence line length. Then, the total weights of all vehicles in the length were divided by the length to obtain the equivalent uniformly distributed load (EUDL). Next, the first truck was deleted, and one or more truck were added to cover the span length. The EUDL distribution was identified by repeating the procedure. The maximum EUDL during the measured period of WIM data was calculated and the lane load model was proposed based on it.

The two lane load model assumed traffic jam situation. However, the traffic jam situation is not always expected to occur, but in a special cases like traffic accident or holiday events. Traffic jam assumption without considering the probability of occurrence may lead to unnecessary conservative design. Therefore, the load model should reflect the actual traffic. In this chapter, the drive analysis method, which investigates the actual traffic based on WIM data, was proposed. And a method for developing multiple presence factors appropriate for long span bridges based on the drive analysis was proposed.

4.2 Weight-In-Motion data

The WIM system collects axle weights without interrupting traffic. Therefore, the reliable traffic data can be collected without artificial bias such as controlling lift axles or avoiding checkpoints. The WIM data used in this paper was provided by the Korean Expressway & Transportation Research Institute. And data used by Hwang (2008) and Lee (2014) was also used. The WIM data includes gross vehicle weight (GVW), axle weight, axle spacing, time, driving lane, speed, vehicle type, etc.

4.2.1 WIM locations

Traffic patterns vary depending on regions and road classifications. Therefore collecting WIM data from various locations is important. The measured WIM data used in this paper is presented in Table 4.1. Data of all lanes in both directions is preferable, but the WIM data collected is only one-directional data.

The quality of information is more important than the quantity of data collected. WIM equipment should be calibrated regularly and collected data should be carefully monitored. WIM data was calibrated with respect to temperature difference between the top and bottom of pavement and about wheel position. Kwon et al. (2010) and Hwang (2008) described the detailed algorithm of the calibrations.

Shivakumar et al. (2011) recommended use of a year's worth of recent continuous data or at least one month of data for each season for each site to observe seasonal variation. Therefore, WIM data for the sites measured in the long term, GC, SS, WG, PH (2010~11), were focused.

Table 4.1 WIM measurement locations

Site	# of WIM Lanes (one Direction)	Date	# of Vehicle data
Gimcheon (GC)	3	2013.01.31 ~ 12.31	4,221,557
Seonsan (SS)	2	2013.01.22 ~ 12.31	8,212,839
Waegwan (WG)	4	2013.01.31 ~ 12.29	15,896,920
Pohang (PH)	2	2010.05.24 ~12.31	1,211,810
		2011.01.01 ~ 12.13	
Yeoju (YJ)	2	2006.05.13 ~ 06.06	29,400
		2010.10.11 ~ 10.25	66,929
		2005.01.12~04.28	314,183
Munmak (MM)	1	2006.10.24~12.01	10,151

4.2.2 Data Scrubbing

The quality of WIM data is more important than quantity in the development of the live load model. WIM system collects data from high-speed traffic that the collected WIM data need to be reviewed or monitored. To edit “bad or unreliable data” out of WIM data, Shivakumar et al. (2011) used data scrubbing rules. Data scrubbing rules should consider differences in traffic characteristics of the site. In this paper, the WIM data is scrubbed using the following filters:

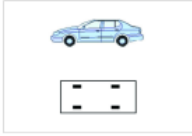
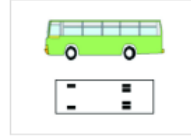
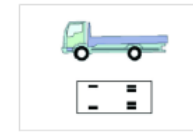
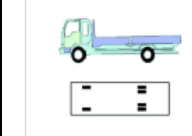
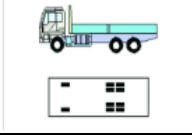
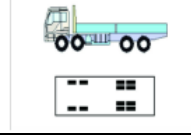
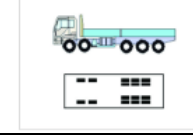
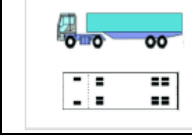
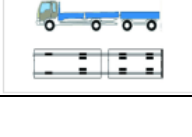
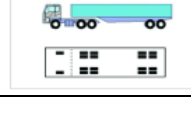
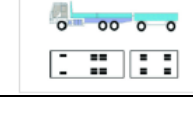
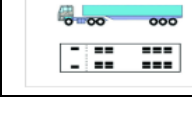
- The number of axles < 2
- Records with the number of axles ≥ 9 are considered to have 8 axles
- Records where the sum of axle spacing is greater than 40m, or the steer axle spacing is greater than 20m
- GVW is 0 ton or negative value

- Records where GVW > 100 ton
- Records where the steer axle weight is > 15 ton
- Records where one axle weight is greater than 20 tons and greater than 60% of GVW at the same time
- Records from a single not fully recorded for 24 hours

4.2.3 Data generation

The GC, SS, WG WIM data includes all vehicle types, though the other sites collected only data on heavily loaded trucks with certain lower weight limit. WIM data of these sites are assumed to have only Types 3~12, and the Type 1 and 2 data was generated based on average traffic ratio from 1995~2013 (MLTM, 2004; 2008; 2013). The vehicle type classification is shown in Table 4.2.

Table 4.2. Twelve vehicle type classifications (MLTM, 2012)

<p>Type 1 (passenger car)</p> 	<p>Type 2 (bus)</p> 	<p>Type 3 (small truck A)</p> 	<p>Type 4 (small truck B)</p> 
<p>Type 5 (medium truck A)</p> 	<p>Type 6 (medium truck B)</p> 	<p>Type 7 (medium truck C)</p> 	<p>Type 8 (large truck A)</p> 
<p>Type 9 (large truck B)</p> 	<p>Type 10 (large truck C)</p> 	<p>Type 11 (large truck D)</p> 	<p>Type 12 (large truck E)</p> 

The data generation procedures are based on the assumption of random traffic situation. The generated vehicles are assumed to travel with the same velocity as the first truck in front of the generated vehicle. The procedures of data generation are as follows:

- The WIM time record of heavy trucks is kept as recorded in WIM
- Generate vehicles type I and II in accordance with the following traffic ratio assumption and assumed properties presented in Table 3.3

(Type 1) : (Type 2) : (the others) = 63 : 7 : 30
- Determine the number of generated vehicles between two measured trucks randomly based on the random traffic situation assumption
- Determine the time information of generated vehicles
 - if the generated vehicles between two trucks satisfy the safety distance within the two trucks, the generated vehicles equally divide the time gap of two trucks
 - if the generated vehicles between two trucks do not satisfy the safety distance between the two trucks, move one by one of the generated vehicles behind the next truck until safety distance is satisfied.
 - the safety distance is in proportional to the square of velocity and the safety distance at 100km/h is 100m.

Table 4.3 Properties of the generated data

Generated vehicle type	# of axle	Axle spacing [cm]	GVW* [kg]
Type 1	2	275	1,000 ~ 2,000
Type 2	2	550	12,000 ~ 15,000

GVW of generated data was determined randomly from uniform distribution of GVW* by random sampling.

Axle weights are assumed to have 50% of the GVW each.

4.2.4 Statistics of collected data

WIM data after scrubbing and data generation procedure is presented in Table 4.4. To consider seasonal or other variation, WIM data including at least one month each season, GC, SS, WG, PH (2010~11), were selected for further analysis.

There are several factors that affect vehicular live load. AASHTO LRFD (2012) applies different multiple presence factors for different ADTT (Average Daily Truck Traffic). According to Nowak et al. (2010), the live loads for long spans depend on the mix of traffic and headway distance. The basic traffic characteristics were investigated. Daily traffic volume in a lane and the average GVW of vehicle types in different WIM locations are compared in Figures 4.3 and 4.4. And the average speed is compared in Table 4.5.

Table 4.4 WIM data after scrubbing and data generation

Site	# of WIM Lanes (one Dir)	# of WIM days	ADT	ADTT
GC	3	236	17,885	5,649
SS	2	276	29,484	8,657
WG	4	295	53,595	15,201
PH (2010~11)	2	402	8,525	2,560
PH (2006)		21	4,197	1,255
YJ (2010)	2	14	15,894	4,778
YJ (2005)		79	12,374	3,720
MM	1	19	1,260	378

ADT: Average Daily Traffic, ADTT: Average Daily Truck Traffic

Average daily traffic and truck traffic in one lane were large in SS and WG. And the average GVW of heavy trucks (type 7, 12) in GC, SS was heavier than others. The average speed was the lowest at PH (2010~11), but still higher than 70km/h, which implies that the traffic jam situation is not typical traffic condition in reality.

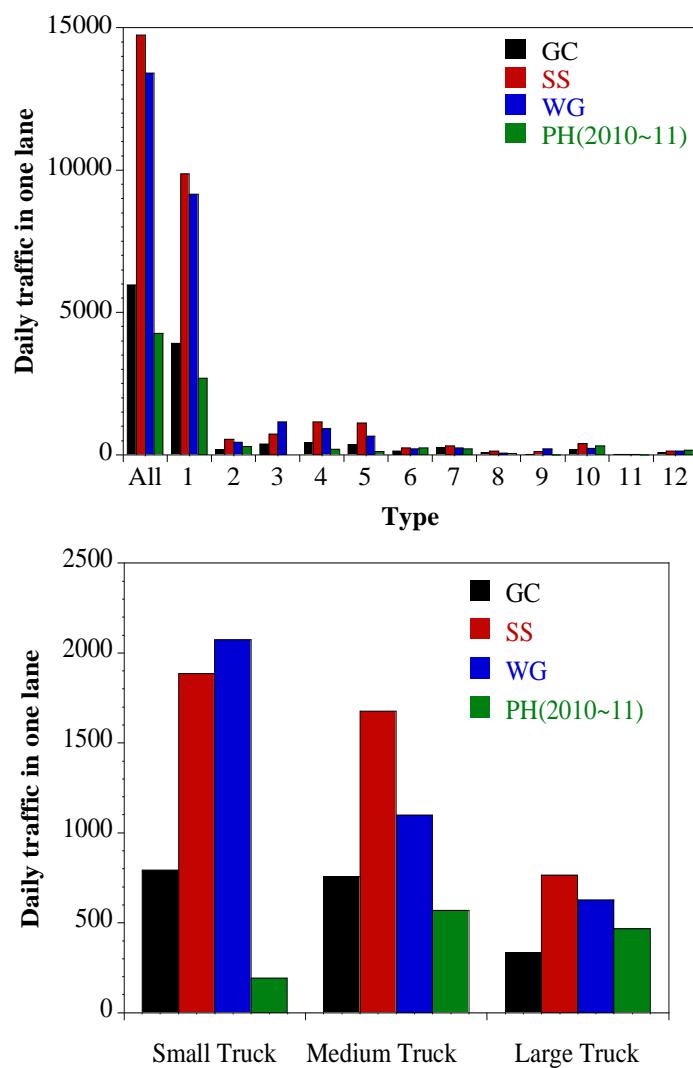


Figure 4.3 Average daily traffic of each vehicle type and truck traffic in one lane

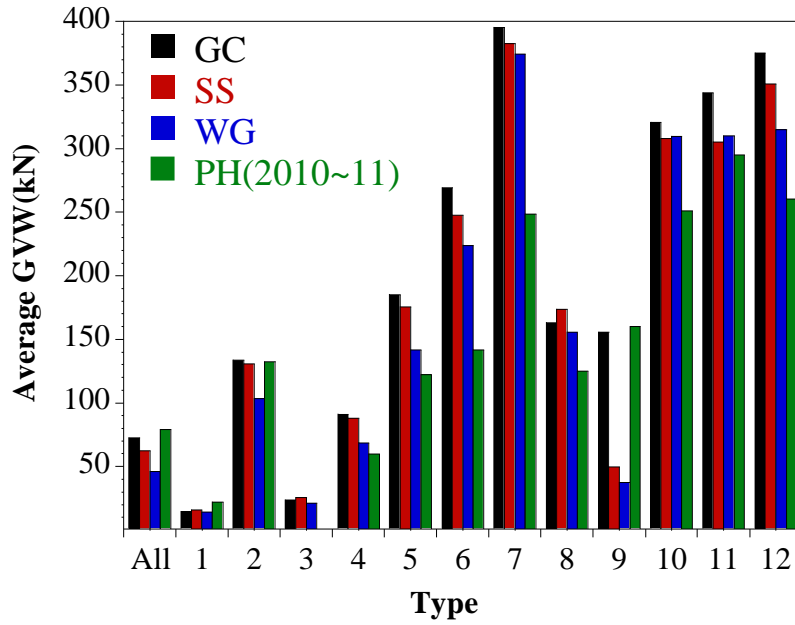


Figure 4.4 Average GVW of each vehicle type

Table 4.5 Speed statistics of WIM data

Site	Speed (km/h)	
	Average	Standard Deviation
GC	93.29	14.7
SS	91.49	16.6
WG	93.08	13.5
PH (2010~11)	76.27	12.3

4.3 Drive Analysis

Nowak et al. (2010) and Hwang (2012) developed a live load model for long span bridges assuming the occurrence of traffic jam situation. However, the average traffic speed measured is higher than 70km/h, indicating that traffic jams seem to be rare. The live load model based on severe situation assumption may lead to unnecessary conservatism. Therefore, realistic traffic situations need to be investigated, so driving situations were analyzed using recently measured WIM data.

4.3.1 Method

It was assumed that the actual traffic flow could be modeled by the WIM data. The WIM data includes the measured time, axle weights, axle spacing, speed, lane, vehicle type, etc. It was assumed that vehicles maintain the same speed and lane when driving, and that the location of the steer axle of vehicles was right on the entrance of bridge when it was measured by the WIM system. The procedure of the drive analysis is as follows:

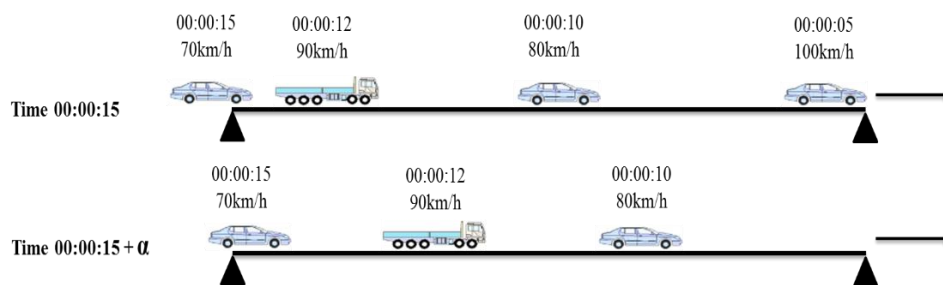


Figure 4.5 Vehicle position of a certain time

- 1) Vehicle location at a certain time is calculated based on the speed and measured time data as described in Figure 4.5 (data on the vehicle figures are the measured time and velocity information of each vehicle. The time at the very left is the reference time according to which vehicles are arranged)
- 2) Calculate the total axle weights on the bridge length
- 3) Calculate representative uniformly distributed load (UDL)

$$\text{UDL} = \frac{\text{total axle weights on the bridge length}}{(\text{length of the bridge}) \times (\text{number of lane})} \quad (4.1)$$

- 4) Repeat steps 1) ~ 3) when an axle passes through the bridge entrance
- 5) Repeat steps 1) ~ 4) using different bridge lengths

4.3.2 Results

The UDLs are the average with regard to the number of lanes and they are assumed to be representative values of whole-lane traffic at each time. The results of drive analysis with the WIM data were presented in Tables 4.6 ~ 8. The average of the UDL decreased when the length increased. The maximum UDL was bigger than the sum of the average and exhibited at standard deviation of six. This means that the UDL value near the maximum happens rarely compared to all events. There are some severe loads, but ordinary traffic is very low compared to the severe loads.

Table 4.6 The average of UDL (kN/m)

Length (m)	GC	SS	WG	PH (2010~11)
250	0.35	0.67	0.42	0.56
500	0.30	0.60	0.40	0.49
750	0.29	0.57	0.39	0.46
1000	0.28	0.56	0.38	0.44
1250	0.27	0.55	0.38	0.43
1500	0.27	0.54	0.38	0.43
1750	0.27	0.54	0.38	0.42
2000	0.26	0.54	0.38	0.41

Table 4.7 The standard deviation of UDL (kN/m)

Length (m)	GC	SS	WG	PH (2010~11)
250	0.36	0.55	0.32	0.47
500	0.26	0.42	0.25	0.36
750	0.22	0.37	0.22	0.32
1000	0.20	0.34	0.21	0.29
1250	0.19	0.32	0.20	0.28
1500	0.18	0.31	0.19	0.27
1750	0.17	0.30	0.18	0.26
2000	0.16	0.29	0.18	0.25

Table 4.8 The maximum value of UDL (kN/m)

Length (m)	GC	SS	WG	PH (2010~11)
250	4.28	6.22	3.42	5.91
500	2.62	4.97	2.95	4.16
750	2.53	4.61	2.59	3.11
1000	2.22	4.42	2.48	2.77
1250	2.27	4.20	2.58	2.44
1500	2.11	3.99	2.51	2.22
1750	2.06	3.89	2.60	2.14
2000	1.91	3.58	2.56	2.06

4.4 Multiple Presence Factor

The UDLs are the average uniformly distributed load with regard to the number of lanes. And those of UDLs were assumed to be the representative lane load of single lane traffic at each considered time. Therefore multi-lane traffic at each considered time can be modeled by multiplying the UDLs by the number of lanes. But the multi-lane reduction effect has to be considered. The multi-lane reduction effect can be defined by equation (4.2):

$$\text{Reduction factor} = \frac{\text{The average of the max. load of the whole lane}}{\text{The max. load of one lane}} \quad (4.2)$$

4.4.1 Method

Let the UDL values of each site from drive analysis of WIM be the population of the lane load of each site. Each UDL value is the average lane load at a specific time, which describes the traffic situation at that time. Therefore multi-lane driving simulations can be performed by sampling UDLs from the population for each lane. The multi-lane driving simulations are described in Figure 4.6. Then, multiple presence factors were proposed according to the following procedures:

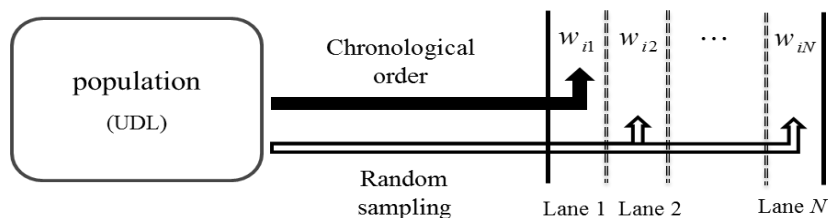


Figure 4.6 Multi-lane simulation

- 1) Assemble population data, UDL, according to the drive analysis described in section 4.3
- 2) Select a single value (ω_{i1}) for lane 1 from the population in chronological order
- 3) Select a single value for lanes 2~8 ($\omega_{i2} \sim \omega_{i8}$) each from the population by random sampling without considering time sequence
- 4) Repeat steps 2), 3) as many as the size of the population
- 5) Calculate the multi-lane reduction ratio using equation (4.3)
- 6) Repeat steps 2) ~ 5) 1,000 times and select the ten largest values (upper 10% value) of the ratio as multiple presence factors

$$\text{reduction ratio} = \frac{\max\left(\sum_{j=1}^N \omega_{ij}\right)}{\max(\omega_{i1})} \quad (4.3)$$

where, N is the number of total lanes, ω_{ij} is the lane load of lane j at i -th time sequence

4.4.2 Proposal of multiple presence factor for bridges with long spans

The multiple presence factors were estimated for 100, 300, 500, 1000m of GC, SS, WG, PH (2010~11) and proposed based on the average values of GC, SS, WG, PH (2010~11). The UDLs were already averages with regard to the number of lanes, such that the UDLs were assumed to be two-lane averages and, therefore, the multiple presence factors of two loaded lanes were normalized to 1.0. The results were compared with KBDC (2012) and AASHTO (2012) in Table 4.9 and Figure 4.7.

The multiple presence factors of KBDC (2012) were divided by the multiple presence factor value of 2 loaded lanes for direct comparison. The load reduction effect of the proposed multiple presence factor was less than that of KBDC (2012) and similar to AASHTO (2012) for loaded lanes 1~4. More radical multiple presence factors were proposed, providing decreasing values up to loaded lane 6.

Table 4.9 Multiple presence factors

Loaded Lanes	KBDC*	AASHTO	Proposed	Average of GC, SS, WG, PH (2010~11)			
				100m	300m	500m	1000m
1	1.0 (1.11)	1.20	1.25	1.30	1.27	1.22	1.23
2	0.9 (1.00)	1.00	1.00	1.00	1.00	1.00	1.00
3	0.9 (0.89)	0.85	0.80	0.78	0.81	0.79	0.78
4	0.7 (0.78)	0.65	0.70	0.66	0.69	0.67	0.67
5	0.65 (0.72)	0.65	0.60	0.58	0.62	0.60	0.59
6	0.65 (0.72)	0.65	0.55	0.53	0.56	0.55	0.54
7	0.65 (0.72)	0.65	0.55	0.49	0.51	0.51	0.50
8	0.65 (0.72)	0.65	0.55	0.45	0.49	0.47	0.48

The KDBC* values in parentheses are normalized to 1.0 for two lanes

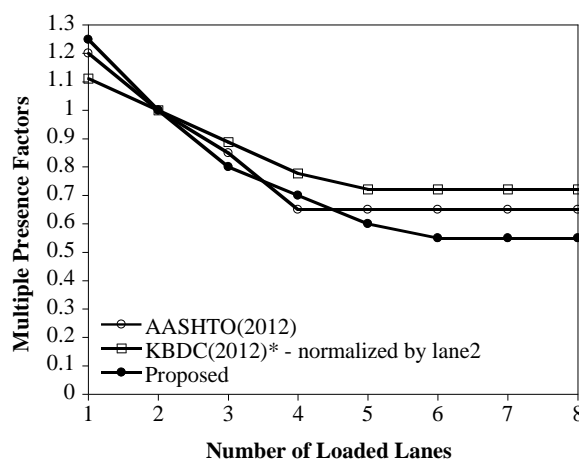


Figure 4.7 Comparison of the multiple presence factors (The KDBC (2012)* is normalized to 1.0 for two lanes)

5. Statistical Model of Live Load for Long span Bridges

Identification of a statistical model of vehicular live load is essential for probability-based design code. The variation is described by distribution type, bias factor, and coefficient of variation. In Korea, the statistical characteristics of short-to medium-span bridges is presented by Hwang (2008; 2012). But for longer-span bridges, those have not been clearly stated. Hwang (2012) developed the lane load model for long span cable bridges but did not provide its statistical characteristics. Lee (2014) estimated the bias factor of the lane load, which was excessive compared to the bias factor of the KBDC (2012).

The reason for this excessive bias may be the assumed traffic jam. Indeed the speed results of WIM showed that traffic jams are rare case in reality. Therefore, the statistical characteristic was again estimated by drive analysis.

Lee (2014) used statistical extrapolation method for estimating maximum load over the design period, compared to the Hwang's (2012) method of using the maximum value of the measured period without extrapolation. The statistical extrapolation method was also investigated to evaluate whether it affected the excessive bias factor result.

5.1 Estimation of the Maximum Load

The time period should be defined in order to devise the statistical model of vehicular live load. To estimate the probability of bridge failure during the design period, the magnitude of maximum load should be calculated. The design of bridges requires the estimation of the maximum load effect during the design period, such as 100 years for KDBC and 75 years for AASHTO LRFD. It is impossible to collect sufficient data to identify the maximum load effect in a 75-year or 100-year period and, therefore, statistical projection should be performed. In this paper, maximum load was considered instead of maximum load effect based on an assumption that load and load effect have a linear relationship.

5.1.1 Estimation by return period load

(1) Return period

If a process is stationary, the return period T of a given event x_T is defined as the average time elapsing between two successive realizations of the event (x_T) itself and can be expressed as a function of a probability distribution F_X and the average waiting time u_T between two events x (Renata et al., 2012). The return period of a given event x_T can be calculated by equation (5.1).

$$T = \frac{u_T}{1 - F_X(x_T)} \quad (5.1)$$

The design live load model can be determined from the return period load. Return period load can be calculated from the return period and probability distribution. A load distribution can be estimated by field measurement such as WIM. And the probability of exceedence corresponding to the return period can be calculated. The correspondent position of the probability of exceedence in the load distribution is the return period load.

(2) Previous research – Nowak (1999)

The HL-93 live load model is based on the 75-year return period load. Nowak (1999) estimated the 75-year mean maximum load effects, assuming the largest 20% of the whole measured data as a normal distribution. This calculation is based on the assumption that all measured data do not follow a normal distribution, but the tail end of the data resembles a theoretical normal distribution.

To describe the extrapolation procedure, the 100-year mean maximum UDL of GC (500m) was calculated using the extrapolation method of Nowak (1999). The UDLs of GC (500m) data were collected as described in section 4.3 and sorted in increasing order. The empirical CDF is calculated by equation (5.2), and the data was plotted in the normal probability paper as shown in Figure 5.1.

$$F_x(x_m) = \frac{m}{N+1} \quad (5.2)$$

Table 5.1 Number of events and probability according to time period
[Nowak's (1999) method]

Time period T	Number of Events N	Exceedence Probability $1/(N+1)$	Empirical CDF $N/(N+1)$	Inverse Normal S
1 day	8,525	1.173×10^{-04}	0.9998827146	3.679
1 month	255,756	3.910×10^{-06}	0.9999960900	4.470
1 year	3,111,703	3.214×10^{-07}	0.9999996786	4.978
50 years	155,585,154	6.428×10^{-09}	0.9999999936	5.688
100 years	311,170,308	3.214×10^{-09}	0.9999999968	5.805

It was assumed that the load distribution does not change with time. The expected number of events, probability, and the inverse normal was calculated in Table 5.1. Then, the approximate normal distribution was estimated by drawing a straight line fitted to the largest 20% of data as shown in a continuous line. The mean and standard deviation from the fitted to the upper 20% normal distribution are computed in equation (5.3).

$$S_{Data(Top\ 20\%)} = (2.16443)X - (0.15401) = \frac{1}{\sigma_X} X - \frac{\mu_X}{\sigma_X} \quad (5.3)$$

$$\mu_X = 0.1067, \quad \sigma_X = 0.6930$$

The 100-year mean maximum UDL was predicted from equation (5.4), which is the inverse form of equation (5.3). The expected maximum UDL of different design life is the horizontal axis value of the intersection points between the continuous line

and dotted line of each design period (Figure 5.1). The estimated maximum UDLs are shown in Figure 5.1 and Table 5.2.

$$X = \sigma_X S_{Data(Top\ 20\%)} + \mu_X = (0.6930)S_{Data(Top\ 20\%)} + (0.1067) \quad (5.4)$$

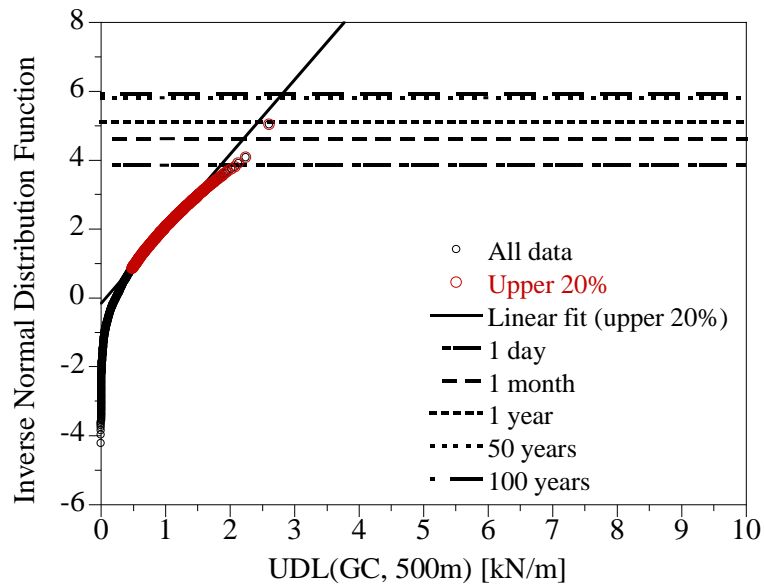


Figure 5.1 Maximum UDL estimation using the extrapolation method of Nowak (1999)

Table 5.2 Maximum UDL estimation [Nowak's (1999) extrapolation method]

Time period T	Inverse Normal S	Estimated Maximum UDL [kN/m]
1 day	3.679	1.856
1 month	4.470	2.208
1 year	4.978	2.436
50 years	5.688	2.757
100 years	5.805	2.810

The mean maximum estimated by Nowak's (1999) method is the UDL, which corresponds to the probability of exceedence of each time period in the load distribution and therefore it is the return period load.

This extrapolation method assumed the upper 20% data as a normal distribution, but it may not be appropriate to use it as a maximum value distribution. The approximated normal distribution changes depending on what percentage of upper data we use. And the maximum load distribution, rather than entire load distribution, is of concern to evaluate the reliability of structure over design life. It is known that extreme value distribution is more appropriate for the maximum value selected from the population.

5.1.2 Estimation by maximum load distribution

(1) Maximum load distribution

The maximum load can be estimated from maximum value distribution. If the sample size is big enough, the maximum value distribution from a population converges to the three types of extreme value distribution as described in section 2.3. Then, the return period load is in the position of the location parameter of extreme value distribution. Equation (5.5) is the nonexceedence probability of return period load (x_T) in initial distribution (F_X). From equation (2.8), the nonexceedence probability of return period load (x_T) in maximum value distribution can be expressed as equation (5.6).

$$F_X(x_T) = 1 - \frac{1}{N} \quad (5.5)$$

$$F_{X_T}(x) = [F_X(x)]^N = \left[1 - \frac{1}{N}\right]^N \stackrel{N \rightarrow \infty}{=} \frac{1}{e} \approx 0.3679 \quad (5.6)$$

N : the expected number of events over period T

The location parameter of extreme value distribution has the same nonexceedence probability as shown in equation (5.7), if the number of events is large enough. Therefore, design load can be proposed by the location parameter in maximum load distribution as the same philosophy of return period load.

$$\begin{aligned} \text{Type I} \quad F_{X_n}(x) \Big|_{x=u_n} &= \exp[-\exp\{-\alpha_n(u_n - u_n)\}] = \frac{1}{e} \\ \text{Type II} \quad F_{X_n}(x) \Big|_{x=v_n} &= \exp\left\{-\left(\frac{v_n}{v_n}\right)^k\right\} = \frac{1}{e} \\ \text{Type III} \quad F_{X_n}(x) \Big|_{x=w_n} &= \exp\left\{-\left(\frac{\omega - w_n}{\omega - w_n}\right)^k\right\} = \frac{1}{e} \end{aligned} \quad (5.7)$$

(2) Previous research – Lee (2014)

Lee (2014) estimated maximum load distribution over the design period using measured maximum load distribution over unit measured time period using the concept of ISO2394 (ISO, 1998). Then, he predicted the maximum load value from the estimated maximum distribution. He assumed the daily maximum values as the Gumbel distribution.

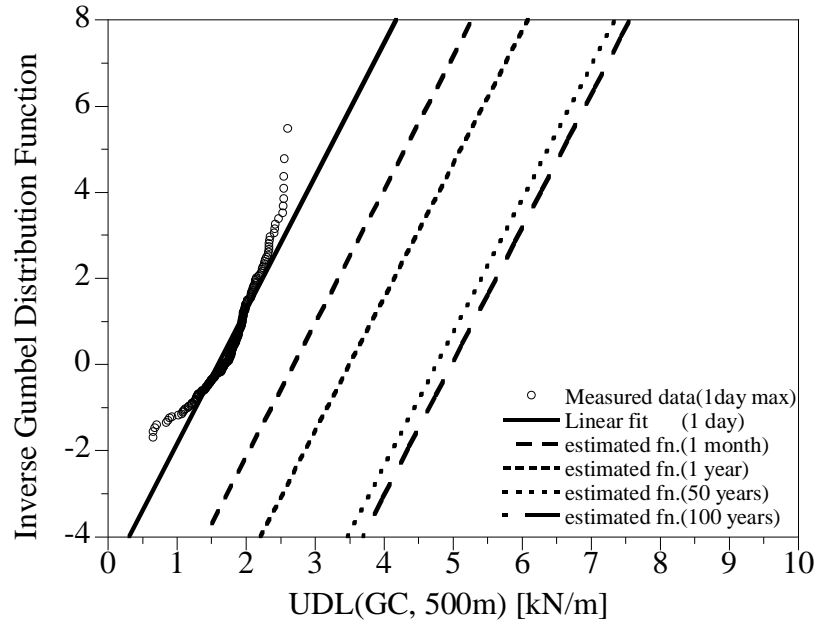


Figure 5.2 Maximum UDL estimation using the extrapolation method of Lee (2014)

To describe the details of the procedure, the 100-year maximum UDL distribution of GC (500m) was calculated using the extrapolation method of Lee (2014). One-day maximum UDLs were collected and sorted in increasing order. The number of daily maximum events, N , is the number of days of the design period. The empirical CDF was calculated by equation (5.2), and the data was plotted in the Gumbel probability paper as described in section 2.3.3. Then, the daily maximum load distribution was estimated by drawing a straight line fitted to the data on the Gumbel probability paper as shown in a continuous line in Figure 5.2.

The location (u_1) and shape parameter (α_1) of daily maximum UDL can be calculated from the fitted line using equation (5.8).

$$\begin{aligned}
S_{Data(Daily\ Max)} &= (3.0983)X - (4.9184) = \alpha_1 X - \alpha_1 u_1 \\
u_1 &= 1.5877, \quad \alpha_1 = 3.0978
\end{aligned} \tag{5.8}$$

The maximum load distribution (F_{x_T}) of design period, T , and the corresponding parameters (u_T, α_T) can be calculated from the daily maximum distribution (F_1) using equations (5.9) and (5.10). And the estimated maximum UDL distribution of the design period, T , was described on the Gumbel probability paper in Figure 5.2. The mean and coefficient of variation can also be calculated from the maximum distribution according to the equation (2.21c).

$$\begin{aligned}
F_{x_T}(x) &= \{F_1(x)\}^T = \exp[-\exp\{-\alpha_1(x-u_1)\}]^T \\
&= \exp\left[-\exp\left\{-\alpha_1\left(x-\left(u_T + \frac{\ln T}{\alpha_1}\right)\right)\right\}\right] \\
&= \exp[-\exp\{-\alpha_T(x-u_T)\}]
\end{aligned} \tag{5.9}$$

$$u_{x_T} = u_{x_1} + \frac{\ln T}{\alpha_1}, \quad \alpha_T = \alpha_1 \tag{5.10}$$

5.1.3 Estimation using Cramer's asymptotic solution

Nowak (1999) assumed a normal distribution based on the upper data distribution profile, and predicted the mean maximum load from the initial upper data distribution. But Lee (2014) estimated not only the return period load, but also the

maximum load distribution over the design period using the extreme value distribution theory. The extrapolation results can vary according to assumption such as normal distribution for upper the 20% data or Gumbel distribution for daily maximum data. The extrapolation method posited by Lee (2014) estimated bigger maximum UDL compared to Nowak's (1999) method.

However, the COVs of maximum distribution did not change for different time periods in Lee's (2014) method because of the property of Gumbel distribution. If the normal distribution assumption of Nowak (1999) is correct, the COV of maximum value distribution should decrease when time period increases. If the initial upper tail of the initial distribution is normal distribution, the maximum distribution converges to a Gumbel distribution as explained in section 2.2.2. Then, the daily maximum distribution should be considered as an approximate – not an exact – Gumbel distribution. And the COV of maximum distribution should decrease when design period increases according to the equation (2.24). Therefore, a new extrapolation method estimating maximum load distribution from normal distribution was proposed using Cramer's asymptotic solution.

(1) Cramer's asymptotic solution

If initial random variable X follows the normal distribution of mean μ_{event} and standard deviation σ_{event} , then the maximum value after N repetitions taken

from initial distribution asymptotically approaches an Extreme Value Type I distribution with the parameters shown in equation (5.10) as derived in section 2.2.2.

$$u_N = \mu_{\text{event}} + \sigma_{\text{event}} \left[\sqrt{2 \ln N} - \frac{\ln \{\ln(N)\} + \ln(4\pi)}{2\sqrt{2 \ln N}} \right], \quad (5.10)$$

$$\alpha_N = \frac{\sqrt{2 \ln N}}{\sigma_{\text{event}}}$$

u_N and α_N are the location and shape parameter of maximum value distribution, respectively

(2) Estimation of maximum load distribution by Cramer's asymptotic solution

It is assumed that the upper UDL follows a normal distribution in line with Nowak's (1999) assumption. Then, the daily maximum UDL distribution can be assumed to be a Gumbel distribution if the number of events is large enough. The number of events corresponding to the daily maximum distribution is the ADT, which is normally more than 1,000, that assumed to be large enough for the assumption. The initial UDL distribution can be derived from the daily maximum UDL distribution, and 100-year maximum UDL distribution can also be derived from Cramer's asymptotic solution.

To describe the extrapolation procedure, the 100-year maximum UDL of GC (500m) was calculated using the extrapolation method of Cramer's asymptotic solution. . The daily maximum UDL distribution was estimated according to the same procedure described in section 5.1.2, using Gumbel probability paper. Then, the initial UDL distribution was estimated by equation (5.11).

$$\sigma_X = \alpha_{X_{1day}} \sqrt{2 \ln(ADT)}$$

$$\mu_X = \sigma_X \left[\sqrt{2 \ln(ADT)} - \frac{\ln \{ \ln(ADT) \} + \ln(4\pi)}{2\sqrt{2 \ln(ADT)}} \right] - u_{X_{1day}}, \quad (5.11)$$

μ_X and σ_X are the mean and standard deviation of initial UDL distribution, and $u_{X_{1day}}$ and $\alpha_{X_{1day}}$ are the location and shape parameter of daily maximum UDL distribution, respectively.

Then, the 100-year maximum Gumbel distribution $F_{X_{100year}}$ was derived from the initial normal distribution F_X using equation 5.10, with $N = ADT \times 365 \times 100$. The approximated daily maximum distribution, estimated initial normal distribution, and the estimated 100-year Gumbel distribution of UDL are shown in Figure 5.3. The 100-year return period UDL was 9% lower than Lee's (2014) method, and Figure 5.4 compared the two methods. It was still greater than Nowak's (1999) method, but Nowak's (1999) method underestimated a 100-year return period load with stiffer slope than the trend exhibited by the data as shown in Figure 5.1. The measured maximum UDL was 2.6153 kN/m, and the measured period was 236 days for GC, 500m UDL. The three methods are compared in Table 5.3. Nowak's (1999) method (under)estimated the closest 236-day UDL. The proposed method estimated 236-day UDL more precisely than Lee's (2014) method.

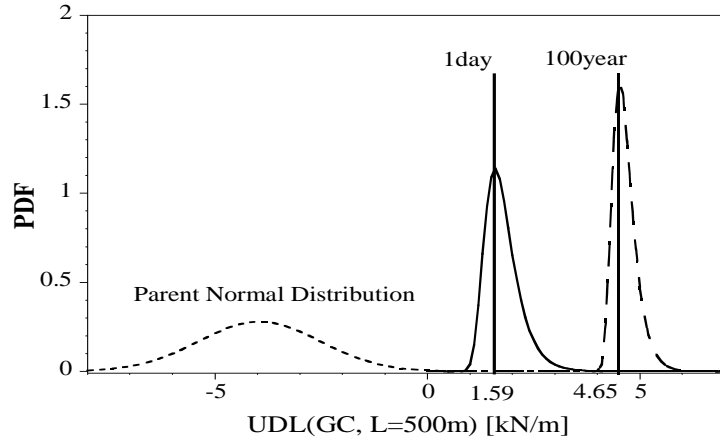


Figure 5.3 Estimated maximum UDL distribution using Cramer's asymptotic solution

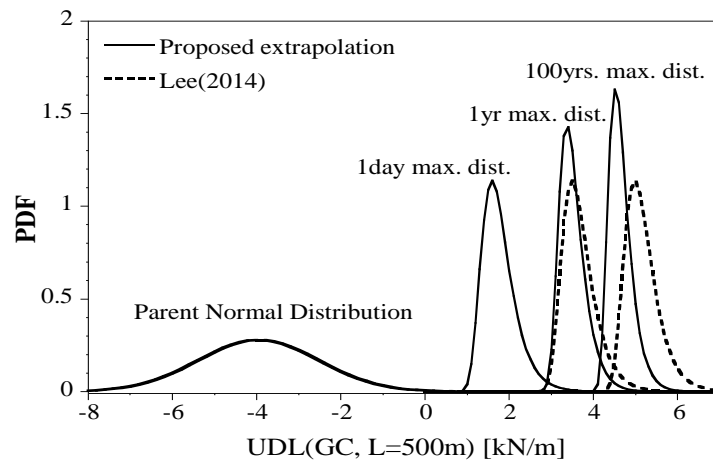


Figure 5.4 Comparison of extrapolation method between the proposed method and Lee's (2014) method

Table 5.3 Comparison of the measured and estimated maximum UDL of GC (500m)

	Measured	Nowak's (1999) method	Lee's (2014) method	Proposed method
236-day Max. UDL [kN/m]	2.615	2.398	3.351	3.254
Error(%)	-	8.30	28.15	24.44

5.2 Statistical Characteristics of Vehicular Live Load

5.2.1 Design live load model

The design live load model of KBDC (2012) consists of a design truck model and design lane load (Figure 5.5, Table 5.4). The extreme load effect is taken as the larger between ‘the effect of one design truck’ and ‘the effect of 75% of design truck combined with the effect of the design lane’.

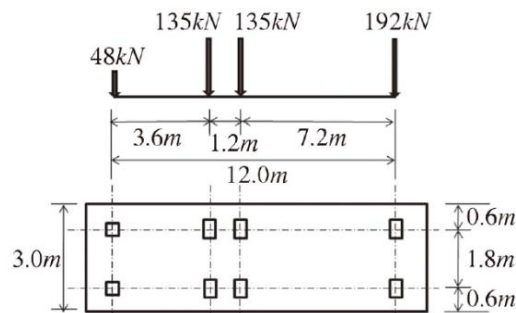


Figure 5.5 Design truck load (KBDC, 2012)

Table 5.4 Design lane load (KBDC, 2012)

$L \leq 60 \text{ m}$	$w = 12.7 \text{ (kN/m)}$
$L \geq 60 \text{ m}$	$w = 12.7 \times \left(\frac{60}{L}\right)^n \text{ (kN/m)}$

A value of 0.18 for n is provided in KBDC (2012). Hwang (2012) proposed a value of 0.15 for a new lane load model for long span cable bridges with the same truck load.

5.2.2 Bias factor of the design lane load model

Bias factor, mean to nominal lane load, was calculated. The mean value was calculated by equation (2.27c) from the 100-year maximum UDL distribution. Nominal lane load is the lane load model of Hwang (2012) multiplied by the two-lane multiple presence factor of 0.9.

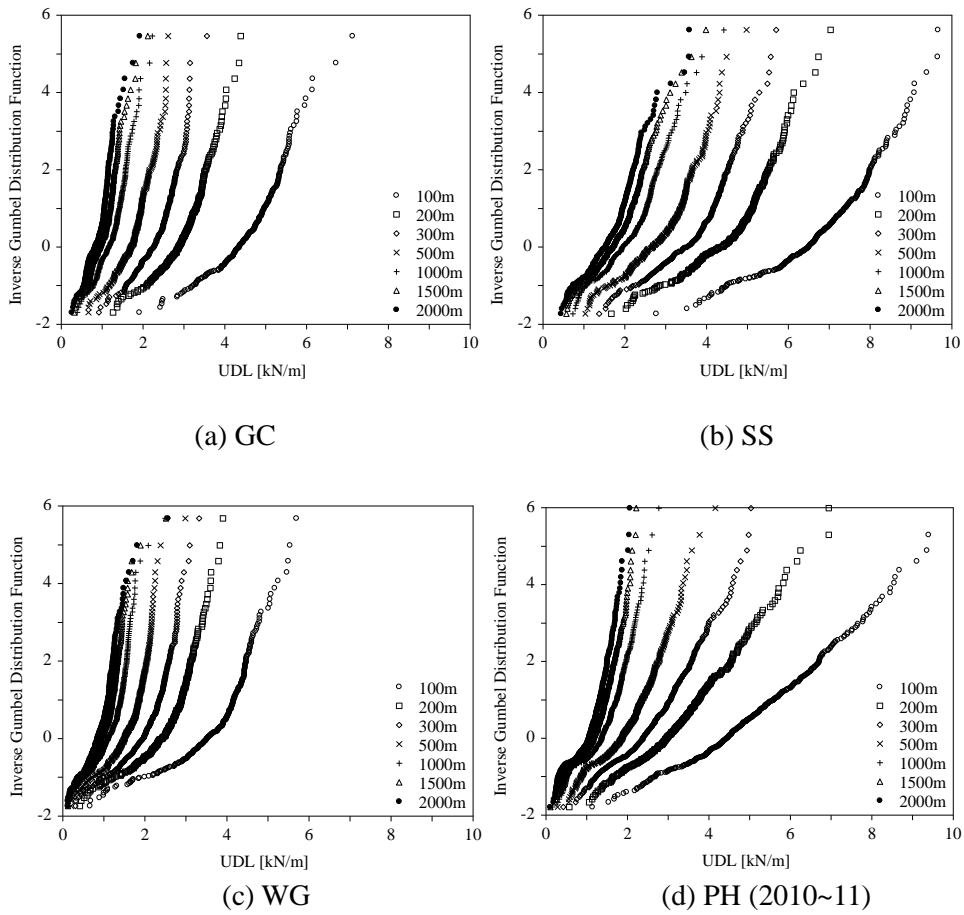


Figure 5.6 Daily maximum UDL distribution

The 100-year maximum UDL distribution was estimated by the proposed method in section 5.1.3 from each site using span lengths of 50, 75, 100, 200, 250, 300, 400, 500, 750, 1000, 1250, 1500, 1750 and 2000m. The daily maximum UDL distribution of four sites was presented in Figure 5.6. The daily maximum UDL distribution, estimated initial UDL distribution, and 100-year maximum UDL distribution results are presented in Tables 5.5 ~ 5.7. UDL decreased as length increased, and the results at the SS site were greater than those of other sites.

Table 5.5 Daily maximum UDL distribution (Gumbel distribution)

Length (m)	Location parameter				Shape parameter			
	GC	SS	WG	PH (2010~11)	GC	SS	WG	PH (2010~11)
50	6.54	9.59	4.97	6.78	0.98	0.69	0.84	0.55
75	5.06	7.36	3.82	5.16	1.25	0.87	1.04	0.71
100	4.16	6.15	3.20	4.29	1.48	0.96	1.23	0.83
200	2.71	4.07	2.16	2.82	2.07	1.21	1.69	1.18
250	2.36	3.59	1.90	2.46	2.25	1.29	1.89	1.30
300	2.12	3.26	1.74	2.22	2.49	1.38	2.02	1.44
400	1.78	2.81	1.51	1.90	2.84	1.48	2.25	1.62
500	1.59	2.52	1.35	1.69	3.10	1.56	2.48	1.79
750	1.27	2.10	1.13	1.37	3.45	1.76	2.86	2.10
1000	1.09	1.86	1.00	1.20	3.77	1.89	3.12	2.35
1250	0.98	1.69	0.91	1.08	4.01	2.01	3.34	2.53
1500	0.90	1.58	0.85	1.00	4.23	2.09	3.53	2.64
1750	0.83	1.49	0.81	0.94	4.40	2.16	3.65	2.76
2000	0.79	1.42	0.78	0.89	4.62	2.23	3.77	2.83

Table 5.6 Estimated parent UDL distribution (Normal distribution)

Length (m)	Mean				Standard deviation			
	GC	SS	WG	PH (2010~11)	GC	SS	WG	PH (2010~11)
50	-10.91	-16.86	-18.04	-21.77	4.50	6.61	5.56	7.72
75	-8.72	-13.59	-14.67	-17.12	3.55	5.23	4.47	6.02
100	-7.47	-12.66	-12.56	-14.66	3.00	4.70	3.81	5.12
200	-5.61	-10.88	-9.25	-10.47	2.14	3.74	2.76	3.60
250	-5.27	-10.46	-8.32	-9.62	1.97	3.51	2.47	3.27
300	-4.77	-9.87	-7.81	-8.74	1.77	3.28	2.31	2.96
400	-4.27	-9.46	-7.07	-7.83	1.56	3.07	2.07	2.63
500	-3.96	-9.12	-6.46	-7.12	1.43	2.91	1.89	2.38
750	-3.71	-8.20	-5.62	-6.12	1.28	2.57	1.63	2.02
1000	-3.47	-7.72	-5.19	-5.49	1.18	2.39	1.49	1.81
1250	-3.31	-7.32	-4.87	-5.14	1.10	2.25	1.40	1.68
1500	-3.16	-7.12	-4.61	-4.96	1.04	2.17	1.32	1.61
1750	-3.07	-6.90	-4.49	-4.76	1.01	2.10	1.28	1.54
2000	-2.93	-6.73	-4.35	-4.66	0.96	2.04	1.24	1.50

Table 5.7 Estimated 100-year maximum UDL distribution (Gumbel distribution)

Length (m)	Location parameter				Shape parameter			
	GC	SS	WG	PH (2010~11)	GC	SS	WG	PH (2010~11)
50	15.78	22.92	15.94	23.11	1.42	0.98	1.18	0.81
75	12.36	17.92	12.64	17.90	1.79	1.23	1.46	1.04
100	10.32	15.63	10.71	15.13	2.13	1.37	1.72	1.22
200	7.11	11.61	7.60	10.43	2.98	1.73	2.37	1.74
250	6.40	10.67	6.78	9.38	3.24	1.84	2.65	1.91
300	5.76	9.87	6.29	8.49	3.59	1.97	2.83	2.11
400	4.99	9.00	5.59	7.47	4.09	2.10	3.16	2.38
500	4.52	8.39	5.07	6.73	4.46	2.22	3.47	2.62
750	3.91	7.29	4.35	5.65	4.96	2.51	4.01	3.09
1000	3.51	6.69	3.95	5.02	5.42	2.69	4.38	3.46
1250	3.25	6.24	3.67	4.64	5.77	2.86	4.68	3.72
1500	3.04	5.96	3.46	4.40	6.10	2.97	4.95	3.88
1750	2.90	5.72	3.33	4.20	6.34	3.07	5.11	4.06
2000	2.76	5.53	3.22	4.07	6.65	3.16	5.28	4.16

Table 5.8 Estimated 100-year maximum UDL distribution (continue)

Length (m)	Mean				COV			
	GC	SS	WG	PH (2010~11)	GC	SS	WG	PH (2010~11)
50	16.19	23.51	16.43	23.83	0.056	0.056	0.066	0.066
75	12.69	18.38	13.04	18.46	0.056	0.057	0.067	0.067
100	10.59	16.05	11.05	15.60	0.057	0.058	0.068	0.067
200	7.30	11.94	7.84	10.76	0.059	0.062	0.069	0.069
250	6.58	10.99	7.00	9.68	0.060	0.064	0.069	0.069
300	5.92	10.17	6.50	8.77	0.060	0.064	0.070	0.069
400	5.13	9.27	5.78	7.71	0.061	0.066	0.070	0.070
500	4.65	8.65	5.24	6.95	0.062	0.067	0.071	0.070
750	4.03	7.52	4.49	5.84	0.064	0.068	0.071	0.071
1000	3.62	6.90	4.08	5.19	0.065	0.069	0.072	0.071
1250	3.35	6.44	3.79	4.79	0.066	0.070	0.072	0.072
1500	3.14	6.15	3.58	4.55	0.067	0.070	0.072	0.073
1750	2.99	5.91	3.45	4.34	0.068	0.071	0.073	0.073
2000	2.85	5.71	3.33	4.21	0.068	0.071	0.073	0.073

The mean value the of 100-year maximum UDL was compared with the nominal value in Figure 5.7. The 100-year UDL decreased when length increased as the design lane load does, however the decreasing rate was stiffer than the design lane load. The bias factor(Figure 5.8) varies from 0.4 to 1.5, which is not uniform for lengths. And the bias factor of SS was more than twice that of GC.

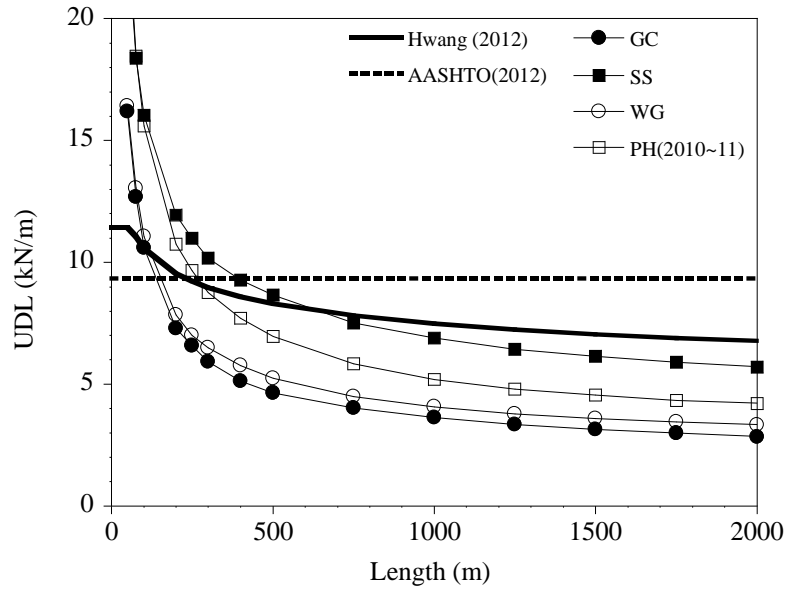


Figure 5.7 The mean value of 100-year maximum UDL

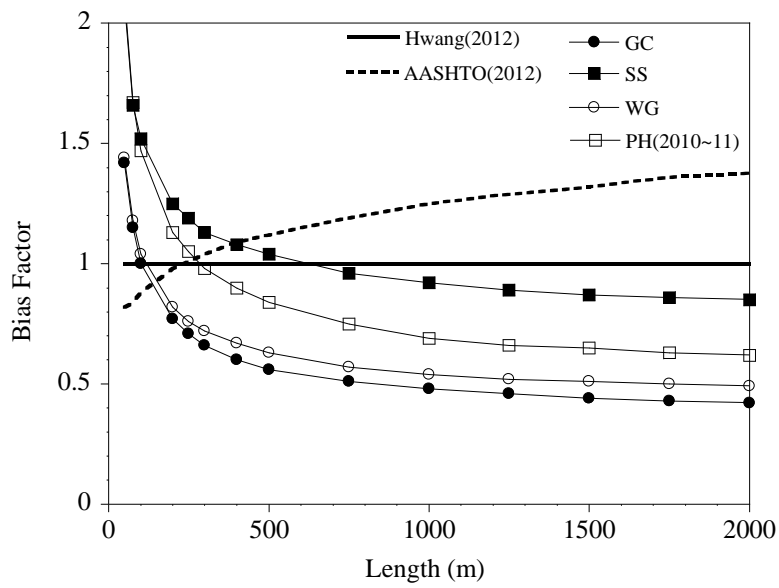


Figure 5.8 Bias factor (mean to nominal value of UDL)

5.3 Proposal of New Lane Load Model

Based on the recently measured WIM data and the drive analysis, the lane load model Hwang (2012) showed non-uniform bias factor according to lengths. And the site-to-site variability should be incorporated. Therefore, a new lane load model was proposed.

5.3.1 Lane load model

(1) Load model for influence line length

A new lane load model was proposed as decreasing in relation to influence line length as shown in equation (5.12). BS5400 and ASCE Report (1981) also used the decreasing form of uniformly distributed load for loaded length. And it is reasonable to define the lane load for influence line length, which is effective loaded length (KSCE, 2006). Parameter A denotes the value of lane load at an influence line length of 100m, and constant lane load was proposed for influence line lengths shorter than 100m, because design truck load effect is dominant for short spans. Parameter B represents the decreasing rate of lane load.

$$w = A \left(\frac{100}{L} \right)^B \quad (5.12)$$

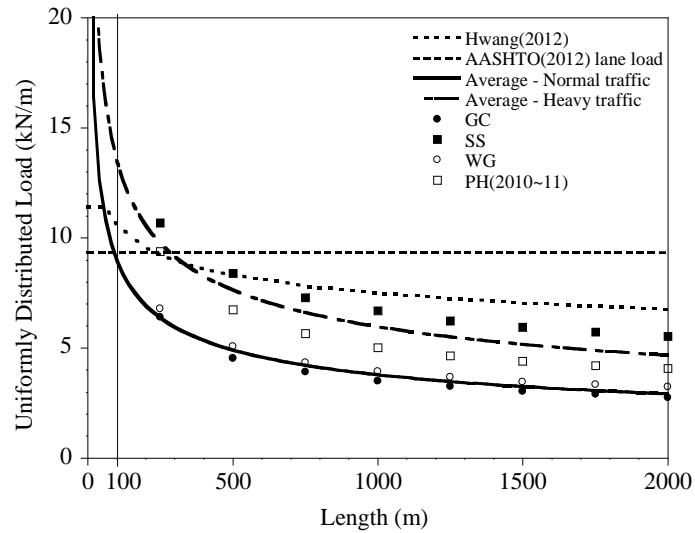


Figure 5.9 Average of normal and heavy traffic lane load

The results were divided into two groups by the magnitude of lane load: normal traffic and heavy traffic. The round markers (GC, WG) were classified as normal traffic and the square markers (WG, PH) were classified as heavy traffic (Figure 5.9). The parameter was fitted for the average return period load of each traffic for 250, 500, 750, 1000, 1250, 1500, 1750, 2000m as shown in Figure 5.9. The proposed value of B , 0.35, was bigger than that used by Hwang (2012) which indicates a faster decreasing rate. The lane load magnitude, A , for normal traffic was close to the AASHTO lane load value and, therefore, the AASHTO lane load value of 9.34 kN/m was proposed. Table 5.9 and Figure 5.10 present data for the proposed lane load model and the mean value of the 100-year maximum UDL distribution of each site.

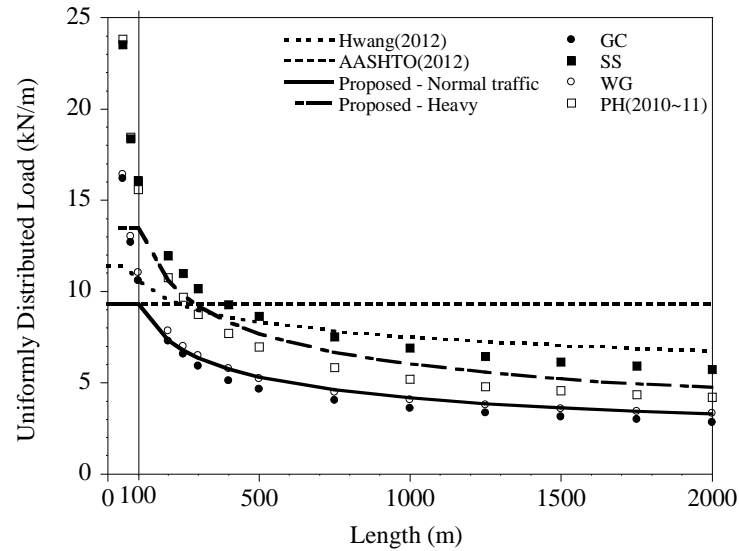


Figure 5.10 Proposed lane load and the mean of 100-year max. UDL

Table 5.9 Proposed lane load, $w = A \times \left(\frac{100}{L}\right)^B$

Parameter	Normal traffic		Heavy traffic		Hwang (2012)
	Fitted from average	proposed	Fitted from average	proposed	
A	8.99	9.34 (AASHTO)	13.52	13.5	11.76
B	0.375	0.35	0.355	0.35	0.15

(2) Load model for span length

Influence line length varies for different member and load effects, that the design procedure can be complicate. KDBC (2014, under revision) offers a more conservative load model for span length that simplifies the design procedure based on Hwang's (2012) load model. Load Model 1 (LM1) is defined in terms of span

Table 5.10 Design lane load (KBDC, 2014 (under revision))

Load Models 1, 2	$L \leq 60$ m	$w = 12.7$ (kN/m)
Load Model 1 (Span length)	$L \geq 60$ m	$w = 12.7 \times \left(\frac{60}{L}\right)^{0.10}$ (kN/m)
Load Model 2 (Influence line length)		$w = 12.7 \times \left(\frac{60}{L}\right)^{0.15}$ (kN/m)

length, and Load Model 2 (LM2) is defined in terms of influence line length (Table 5.10).

For the proposed load model, the span length-based model was also considered with the same conservative level using the weighted geometric mean concept (equation 5.13). The LM1 can be considered as a weighted geometric average between LM2 and the conservative unreduced lane load. The geometric weight used in LM1 was 1/3 as derived in equation (5.14), and this weight was used for the proposed lane load model. The proposed model for span length is presented in equation (5.15).

$$\bar{w} = w_1^\alpha w_2^{1-\alpha} \quad (5.13)$$

$(\alpha \text{ is weight for } w_1, 0 \leq \alpha \leq 1)$

$$\begin{aligned}
w_{LM1} &= w_0^\alpha \times w_{LM2}^{1-\alpha} \\
&= 12.7^\alpha \times \left\{ 12.7 \times \left(\frac{60}{L} \right)^{0.15} \right\}^{(1-\alpha)} \\
&= 12.7 \times \left(\frac{60}{L} \right)^{0.15-0.15\alpha} = 12.7 \times \left(\frac{60}{L} \right)^{0.10}
\end{aligned} \tag{5.14}$$

$\therefore \alpha = 1/3$

$$\begin{aligned}
w_{\text{Normal traffic, span}} &= 9.34^{\frac{1}{3}} \left\{ 9.34 \times \left(\frac{100}{L} \right)^{0.35} \right\}^{\frac{2}{3}} = 9.34 \times \left(\frac{100}{L} \right)^{0.23} \\
w_{\text{Heavy traffic, span}} &= 13.5^{\frac{1}{3}} \left\{ 13.5 \times \left(\frac{100}{L} \right)^{0.35} \right\}^{\frac{2}{3}} = 13.5 \times \left(\frac{100}{L} \right)^{0.23}
\end{aligned} \tag{5.15}$$

where, L is span length(m)

(3) Verification

To verify the proposed model, more WIM data of other sites were compared. The WIM data of PH (2006), YJ (2010), YJ (2005), and MM were used. The mean value of the 100-year maximum distribution is presented in Figure 5.11. The PH (2006), YJ (2010) can be classified as a site of heavy traffic, and the YJ (2005) can be classified as a site of normal traffic. MM is a site of heavy traffic at short spans but normal traffic at longer spans. This is because the traffic is lower than at other sites as presented in Table 4.4. Even though lane load for short spans is high, it can decrease for long spans because of low traffic. MM has to be classified as heavy

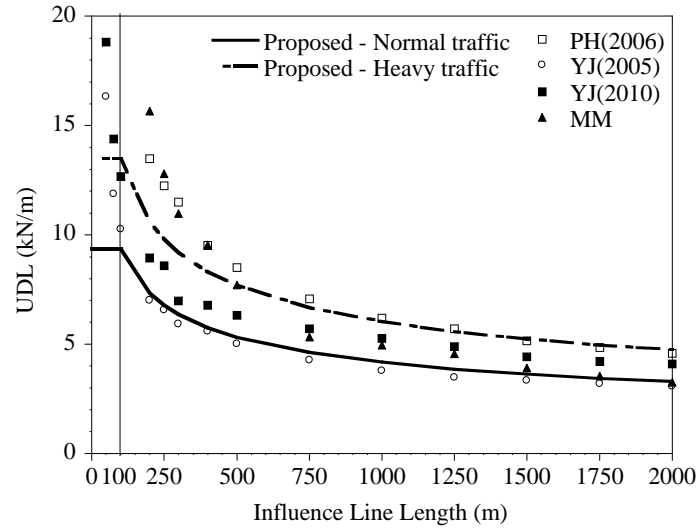


Figure 5.11 Comparison of proposed model with other sites

traffic for conservative design, but we may have to propose a faster decreasing lane load model for regions of low traffic.

The proposed model classifies sites as the normal and heavy traffic sites. But the classification is based on the results of drive analysis, which requires significant computation. Therefore, the standard of classification from objective properties needs to be developed, such as traffic volume, average vehicle weight, average speed, etc.

5.3.2 Statistical characteristics of live load for long spans

The live load model for long span bridges was proposed in section 5.3.1. Statistical characteristics were estimated for the proposed lane load model in this

section. The bias factor of the normal traffic model was 0.87 ~ 1.18, and 0.86 ~ 1.21 for heavy traffic for influence lengths longer than 100m as shown in Figure 5.12. Therefore, bias factor for the proposed lane load model can be proposed as 0.8 ~ 1.2.

Estimated coefficients of variation of 100-year maximum distribution were presented in Table 5.8 and Figure 5.13. The 7% COV was proposed for lane load.

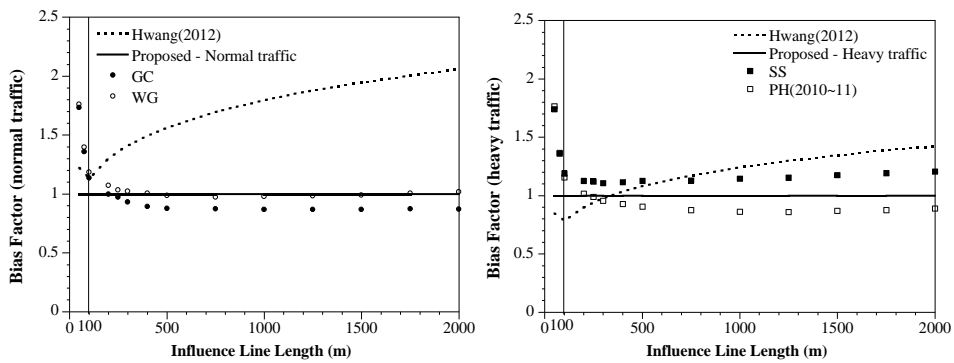


Figure 5.12 Bias factor of proposed lane load model(normal, heavy traffic)

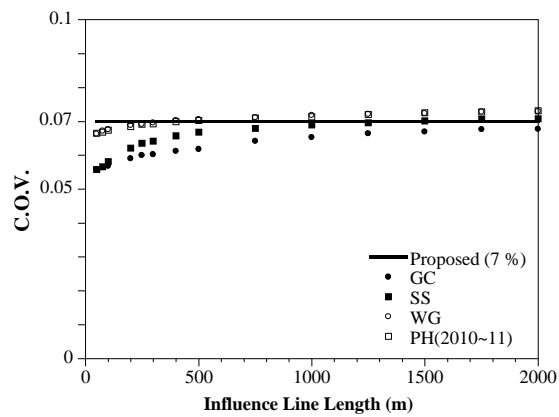


Figure 5.13 Coefficient of variation of lane load

The site-to-site variability and the effect of impact was considered as influence factor (Lee, 2014). The impact was not considered here because the influence of dynamic load is not significant for long spans (Nowak et al., 2010). The bias factor and COV of site-to-site variability was assumed to be 1.0 and 10%, respectively. The site-to-site variability should be investigated using more traffic data, but the same value was assumed to be that from the previous domestic research (Hwang, 2008). The COV could be reduced because the variability was already interpreted by classification of load model as normal and heavy traffic. For the modeling parameter, Hwang (2008) assumed the assumption of Nowak (1999) and Moses (2001); a value of 1.0 for bias factor and 10% for COV.

Considering all these effects, the bias factor for load effect was the same as that of the load model, because the bias factor of the influence factor and modeling parameter are 1.0. Therefore, the bias factor for load effect for long spans can be proposed as 0.8 ~ 1.2. The COV of the load effect for long spans can be proposed as 0.16.

The probability distribution of the influence factor and modeling parameter were assumed to comprise a normal distribution in previous research. The load model was assumed to have a Gumbel distribution according to the drive analysis. A lognormal distribution is known to be appropriate when the variable being modeled is a product of other random variables (Moses, 2001). But if one part exhibits an extreme distribution, it is known that the variable is likely to follow the extreme distribution,

even though the other part of the variable follows a normal distribution (Lee, 2014). Therefore, the load effect was assumed to follow the Gumbel distribution.

5.4 Summary

The statistical model of vehicular live load for long spans was identified. New extrapolation method using Cramer's asymptotic solution was proposed. The estimated 100-year return period UDL showed faster decreasing rate according to length than design load model. Bias factor of lane load model of Hwang (2012) was not uniform according to lengths, and showed site-to-site variability. Therefore, a new live load model for long spans was proposed, considering the decreasing rate and site-to-site variability. The lane load classified into normal and heavy traffic. And the load model for influence line length and span length are proposed. The statistical characteristics of the load model and load effects were identified. The results are summarized as follows:

- Proposed Lane Load – influence line length

$$w_{\text{Normal traffic}} = \begin{cases} 9.34 & L_l \leq 100 m \\ 9.34 \times \left(\frac{100}{L_l}\right)^{0.35} & L_l > 100 m \end{cases} \quad (5.16a)$$

$$w_{\text{Heavy traffic}} = \begin{cases} 13.50 & L_l \leq 100 m \\ 13.50 \times \left(\frac{100}{L_l}\right)^{0.35} & L_l > 100 m \end{cases} \quad (5.16b)$$

- Proposed Lane Load – span length

$$w_{\text{Normal traffic}} = \begin{cases} 9.34 & L \leq 100 \text{ m} \\ 9.34 \times \left(\frac{100}{L}\right)^{0.23} & L > 100 \text{ m} \end{cases} \quad (5.17a)$$

$$w_{\text{Heavy traffic}} = \begin{cases} 13.50 & L \leq 100 \text{ m} \\ 13.50 \times \left(\frac{100}{L}\right)^{0.23} & L > 100 \text{ m} \end{cases} \quad (5.17b)$$

- Statistical Characteristics of Load Effects

- Bias factor : 0.8 ~ 1.2
- COV: 0.16
- Probability distribution: Gumbel distribution

6. Conclusions

The current live load model for long span bridges was developed according to traffic jam scenarios (Hwang, 2012; Nowak et al., 2010). However, the statistical characteristic of the live load model proposed by Hwang(2012) was not clearly stated. Lee (2014) has suggested statistical characteristics of the lane load model of Hwang(2012), but excessive bias factor was estimated, compared to that of KDBC(2012). The traffic jam assumption and the extrapolation method were the reasons for the excessive results. To identify the difference between assumed traffic jam scenario and actual driving situations, recently measured WIM data was interrogated.

To consider actual traffic patterns, driving situations were analyzed. And the multiple presence factor of a live load model for long span bridges was proposed by virtual multi-lane driving simulation using the results from drive analysis. The simulation results showed a greater multi-lane reduction effect than KBDC (2012) and were similar to AASHTO LRFD (2012). A decreasing multiple presence factor for up to six loaded lanes was proposed.

The maximum load distribution was estimated to identify the statistical model of vehicular live load. A new extrapolation method using Cramer's asymptotic solution was proposed to estimate the maximum load distribution. The statistical characteristics of Hwang's (2012) lane load model were identified. Bias factor was not uniform due to different decreasing rates of the 100-year return period load. Site-

to-site variability needed to be considered. A new live load model for long spans was proposed considering the decreasing rate and site-to-site variability. The lane load classified into normal and heavy traffic, and a load model in terms of influence line length and span length were proposed. The statistical characteristics of the proposed load model and load effects were identified.

The proposed model classifies sites into the normal and heavy traffic sites. The standard of classification from objective properties, such as traffic volume, average vehicle weight, average speed etc., are not presented here. Further study is required because the drive analysis requires significant computation.

The proposed load model was developed from WIM data across four sites. More WIM data from many different sites and over a longer period should be analyzed to create a more reliable vehicular live load model.

References

AASHTO (2012) *AASHTO LRFD Bridge Design Specifications*, American Association of State Highway and Transportation Officials, Washington, D.C., USA.

Ang, A. H-S. and Tang, W. H. (1975) *Probability Concepts in Engineering Planning and Design: Volume I – basic Principles*, Wiley & Sons.

Ang, A. H-S. and Tang, W. H. (1984) *Probability Concepts in Engineering Planning and Design: Volume II - Decision, Risk, and Reliability*, Wiley & Sons.

BSI (2003) *Eurocode 1 : Actions on structures*, British Standard Institution, London.

Castillo, E. (1988) *Extreme Value Theory in Engineering*, Academic Press.

Cramer, H. (1946) *Mathematical Methods of Statistics*, Asia Publishing House

Ellingwood, B., Galambos, T. V., MacGregor, J. G., and Cornell. C. A. (1980) *Development of a Probability Based Load Criterion for American National Standard A58: Building Code Requirements for Minimum Design Loads in Buildings and Other Structures*, NBS Special Publication 577, Washington, DC: National Bureau of Standards.

Hwang, E.-S. (2008) *Development of Live Load Model for Reliability-based Bridge Design Code*, Korea Bridge Design & Engineering Research Center, Technical Report Series 034, Seoul, Korea(in Korean).

Hwang, E.-S. (2012) “Development of Live Load Model for Long Span Bridges”, *Economic design technology for long span cable bridge*, Super Long Span Bridge R&D Center, Core Assignment 1, Detail Assignment 1, Research Report, Seoul National University(in Korean).

Hwang, E.-S., Nguyen, T. H., Kim, D.-Y. (2012) “Live Load Models for Reliability-Based Bridge Evaluation”, 18th IABSE Congress, Public Session, pp. 169 ~ 188.

Hwang, E.-S., Nowak, A. S. (1991) “Simulation of Dynamic Load for Bridges”, *Journal of Structural Engineering*, Vol. 117, Issue. 5, pp.1413-1434.

ISO (1998) *International Standard ISO2394: General principles on reliability for structures*, ISO(International Organization for Standardization).

Kang, J. S. (2008) “Detection of Abrupt Changes of Structure using Regularized Autoregressive Model”, Doctoral dissertation, Seoul National University(in Korean).

KSCE (2006) *Design Guideline for Cable Steel Bridge*, Korean Society of Civil Engineers, Seoul, Korea(in Korean).

KRTA(2014) *Korea Bridge Design Code (Limit State Design)- Cable Bridge Design(Draft)*, Korea Road & Transportation Association (in Korean).

Kwon, S.-M. and Lee, K.-H. (2010) “Development of the High-speed Weight-in-motion Systems for Overweight Enforcement in Expressways”, *Journal of Korean Road Association*, Korean Road Association, Vol. 12, No. 2, pp. 45-52(in Korean).

Lee, S. H. (2014) “Calibration of the Load-Resistance Factors for the Reliability-based Design of Cable-supported Bridges”, Doctoral dissertation, Seoul National University(in Korean).

Lutomirska, M. (2009) “Live Load Models for Long Span Bridges”, Doctoral dissertation, University of Nebraska.

MCT (1998) *A study on the development of live and fatigue load model for bridges*, Final Report, Ministry of Construction & Transportation (in Korean)

MLIT (2013) *Annual Traffic Volume Report*, Ministry of Land, Infrastructure and Transport(in Korean).

MLTM (2008) *Statistical Yearbook of Traffic Volume*. Ministry of Land, Transport and Maritime Affairs(in Korean).

MLTM(2012) *Korea Bridge Design Code (Limit State Design)*, Ministry of Land, Transport and Maritime Affairs(in Korean).

MOCT (2004) *Statistical Yearbook of Traffic Volume*. Ministry of Construction & Transportation(in Korean).

Moses(2001), *Calibration of load factors for LRFR bridge evaluation*, NCHRP Report 454, Transportation Research Board, National Academy Press, Washington D.C., USA.

Nowak, A. S. (1993) “Live Load Model for Highway Bridges”, *Structural Safety*, Vol. 13, pp.53-66.

Nowak, A. S. (1999) *Calibration of LRFD Bridge Design Code*, NCHRP Report 368, National Academy Press, Washington, DC., USA.

Nowak, A. S., Hong, Y.-K. (1991) “Bridge Live-Load Models”, *Journal of Structural Engineering*, Vol. 117, Issue. 9, pp.2757-2767.

Nowak, A. S., Lutomirska, M., Sheikh Ibrahim, F. I. (2010) “The development of live load for long span bridges”, *Bridge Structures*, Vol.6, pp73-79.

Nowak, A. S., Nassif, H., DeFrain, L. (1993) “Effect of Truck Loads on Bridges”, *Journal of transportation engineering*, Vol. 119, Issue. 6, pp.853-867

Nowak, A. S., Rakoczy, P. (2013) “WIM-Based Live Load for Bridges”, *KSCE Journal of Civil Engineering*, Vol.17, Issue. 3, pp.568-574.

Shivakuma, B., Chosn, M., Moses, F., and TranSystems Corporation (2011) *Protocols for collecting and using traffic data in bridge design*, NCHRP Report 683, Transportation Research Board, National Academy Press, Washington D.C.

Vezzoli, R., Mercogliano, P. and Pecora, S. (2012) “A Brief Introduction to the Concept of Return Period for Univariate Variables”, Centro Euro-Mediterraneo sui Cambiamenti Climatici, Research Paper 139.

초 록

이 연구에서는 국내의 교통특성을 반영한 장경간 차량활하중의 확률모형을 추정하였다. 기존의 장경간 차량활하중 모형은 실제 교통상황에서 낮은 확률로 발생하는 정체현상을 이미 발생한 것으로 가정하고 있다. 이 가정은 보수적인 설계를 유발할 수 있기 때문에 실제의 교통특성을 고려하기 위하여 최근 측정한 국내 6 개 지역의 통행자료를 이용하여 주행상황을 분석하였다. 설계수명동안의 최대하중을 추정하기 위해 Cramer 의 점근적 해를 이용한 통계적 외삽 기법을 제안하고 기존 방법과 비교하였다. 또한 장경간 하중모형에 적합한 다차로재하계수를 산정하기 위하여 대표차로하중을 구하고 이것을 가상으로 동시주행시켜 다차로재하계수를 산정하는 방법을 제안하였다.

최근 측정한 WIM data 의 주행상황 분석을 통해 황의승(2012)이 제안한 장경간 활하중 모형의 통계특성을 추정하였다. 분석결과 길이에 따른 차로하중의 감소율이 기존 하중모형보다 급격하게 평가돼 길이에 따른 편심계수가 균일하지 않았고, 지역적에 따른 차이 역시 두드러지게 나타났다. 이를 반영하여 새로운 차로하중 확률모형을 제안하였다. 하중 크기에 따라 일반통행(Normal traffic)과 과중통행지역(Heavy traffic)으로

구분하였고, 영향선 길이에 따른 모형과 경간 길이에 따른 모형을 함께 제안하였다. 제안된 하중모형의 통계특성을 함께 제시하였다.

주요어: 장경간 차량활하중, 확률모형, Cramer 의 점근적 해, WIM data,
다차로재하계수

학번: 2013-20924